

1 **Nitrogen cycling in the subsurface biosphere: Nitrate isotopes in**
2 **porewaters underlying the oligotrophic North Atlantic**

3

4 **Scott D. Wankel^{1,*}, Carolyn Buchwald¹, Wiebke Ziebis², Christine B. Wenk^{3,^} and Moritz F.**
5 **Lehmann³**

6 ¹Woods Hole Oceanographic Institution, Department of Marine Chemistry and Geochemistry,
7 266 Woods Hole Rd., Woods Hole, MA, USA 02543

8 ²University of Southern California, Department of Biological Sciences, Allan Hancock
9 Foundation Building, Los Angeles, California, USA 90089

10 ³University of Basel, Department of Environmental Science, Bernoullistrasse 32, Basel,
11 Switzerland CH-4056

12 [^] now at Weizmann Institute of Science, Department of Earth and Planetary Sciences, Rehovot,
13 Israel 76100

14

15 **Running Title:** Nitrogen cycling in deep-sea porewaters

16 **Keywords:** Nitrate, porewater, isotopes, nitrification, denitrification, nitrogen fixation, North
17 Pond, oligotrophic, North Atlantic, IODP

18

19 ***Correspondence:**

20 Dr. Scott D. Wankel
21 Woods Hole Oceanographic Institution
22 Department of Marine Chemistry and Geochemistry
23 266 Woods Hole Rd., MS 25
24 Woods Hole, MA 02543
25 sdwankel@whoi.edu

1 ABSTRACT

2 Nitrogen (N) is a key component of fundamental biomolecules. Hence, the cycling and
3 availability of N is a central factor governing the extent of ecosystems across the Earth. In the
4 organic-lean sediment porewaters underlying the oligotrophic ocean, where low levels of
5 microbial activity persist despite limited organic matter delivery from overlying water, the extent
6 and modes of nitrogen transformations have not been widely investigated. Here we use the N and
7 oxygen (O) isotopic composition of porewater nitrate (NO_3^-) from a site in the oligotrophic North
8 Atlantic (IODP) to determine the extent and magnitude of microbial nitrate production (via
9 nitrification) and consumption (via denitrification). We find that NO_3^- accumulates far above
10 bottom seawater concentrations ($\sim 21\mu\text{M}$) throughout the sediment column (up to $\sim 50\mu\text{M}$) down
11 to the oceanic basement as deep as 90 mbsf, reflecting the predominance of aerobic
12 nitrification/remineralization within the deep marine sediments. Large changes in the $\delta^{15}\text{N}$ and
13 $\delta^{18}\text{O}$ of nitrate, however, reveal variable influence of nitrate respiration across the three sites. We
14 use an inverse porewater diffusion-reaction model, constrained by the N and O isotope
15 systematics of nitrification and denitrification and the porewater NO_3^- isotopic composition, to
16 estimate rates of nitrification and denitrification throughout the sediment column. Results
17 indicate variability of reaction rates across and within the three boreholes that are generally
18 consistent with the differential distribution of dissolved oxygen at this site, though not
19 necessarily with the canonical view of how redox thresholds separate nitrate regeneration from
20 dissimilative consumption spatially. That is, we provide stable isotopic evidence for expanded
21 zones of co-occurring nitrification and denitrification. The isotope biogeochemical modeling also
22 yielded estimates for the $\delta^{15}\text{N}$ and $\delta^{18}\text{O}$ of newly produced nitrate ($\delta^{15}\text{N}_{\text{NTR}}$ and $\delta^{18}\text{O}_{\text{NTR}}$), as well
23 as the isotope effect for denitrification ($^{15}\epsilon_{\text{DNF}}$), parameters with high relevance to global ocean
24 models of N cycling. Estimated values of $\delta^{15}\text{N}_{\text{NTR}}$ were generally lower than previously reported
25 $\delta^{15}\text{N}$ values for sinking PON in this region. We suggest that these values may be, in part, related
26 to sedimentary N_2 fixation and remineralization of the newly fixed organic N. Values of $\delta^{18}\text{O}_{\text{NTR}}$
27 generally ranged between -2.8 and 0.0‰, consistent with recent estimates based on lab cultures
28 of nitrifying bacteria. Notably, some $\delta^{18}\text{O}_{\text{NTR}}$ values were elevated, suggesting incorporation of
29 ^{18}O -enriched dissolved oxygen during nitrification, and possibly indicating a tight coupling of
30 NH_4^+ and NO_2^- oxidation in this metabolically sluggish environment. Our findings indicate that

1 the production of organic matter by in situ autotrophy (e.g., nitrification, nitrogen fixation)
2 supplies a large fraction of the biomass and organic substrate for heterotrophy in these sediments,
3 supplementing the small organic matter pool derived from the overlying euphotic zone. This
4 work sheds new light on an active nitrogen cycle operating, despite exceedingly low carbon
5 inputs, in the deep sedimentary biosphere.

1 1. INTRODUCTION

2 Below the surface ocean, the dark ocean, including environments above and below the
3 seafloor, hosts the largest habitable environment on the planet and is home to a wide range of
4 globally relevant biogeochemical processes (Orcutt et al., 2011). While significant progress has
5 been made in recent years toward characterizing the geological, chemical, and ecological
6 composition of a variety of subsurface environments (Orcutt et al., 2011; Edwards et al.,
7 2011; Edwards et al., 2012b), the potential for impact of these systems on global biogeochemical
8 cycles remains poorly understood. Most of our knowledge about seafloor microbial activity
9 stems from research focusing on productive continental margins, where relatively high fluxes of
10 organic matter from surface primary productivity support a large heterotrophic and mostly
11 anaerobic microbial community, (e.g., (Blair and Aller, 2012)). By comparison, vast areas of the
12 seafloor, in particular those underlying ocean gyres, characterized by low primary productivity
13 and low organic matter flux to the sea floor, have received far less attention (D'Hondt et al.,
14 2009; Mason et al., 2010; Fischer et al., 2009). In contrast to well-studied ocean margin sediments,
15 oxygen (O_2) and nitrate (NO_3^-), two powerful oxidants of organic carbon, penetrate deeply into
16 the sediment underlying oligotrophic ocean waters (D'Hondt et al., 2009; Murray and
17 Grundmanis, 1980; Rutgers van der Loeff et al., 1990; Sachs et al., 2009; D'Hondt et al., 2015; Røy
18 et al., 2012; Fischer et al., 2009). Furthermore, in the sediments overlying relatively young and
19 permeable ocean crust, O_2 and NO_3^- are also supplied via upward diffusion from oxic and
20 nitrate-replete fluids flowing through basaltic basement as has been shown for the North Pond
21 site, which is located on the western flank of the Mid-Atlantic Ridge (Orcutt et al., 2013; Ziebis
22 et al., 2012). At North Pond, where the sediment cover is thin ($< \sim 25$ m), O_2 penetrates the
23 entire sediment column; where sediment thickness is elevated, conditions become anoxic at mid-
24 depths. Aerobic heterotrophic respiration likely dominates organic carbon oxidation in the upper
25 sediment column. However, as organic carbon becomes limiting at greater depths, autotrophic
26 processes (e.g., nitrification) are likely to gain relative importance. Further, there is evidence that
27 the upward supply of oxidants from the basaltic basement supports increased microbial activity
28 (Picard and Ferdeman, 2011). However, a fundamental understanding of the relative importance
29 of specific metabolic activities that drive and sustain subsurface communities is lacking. Because
30 central ocean gyres cover roughly half of the global seafloor, understanding the nature of the
31 biosphere hosted within these sediments may provide important insights into its role in global

1 marine nitrogen and carbon cycling. Here we focus specifically on elucidating subsurface
2 nitrogen cycling and its role in supporting heterotrophic and autotrophic processes in
3 oligotrophic deep-ocean sediments underlying the North Atlantic Gyre, at North Pond (22°45'N,
4 46°05'W).

5 IODP Expedition 336 (Mid-Atlantic Ridge Microbiology, Sept. 16 – Nov. 16, 2011)
6 aimed to directly address the nature of microbial communities in both ocean crust and sediments
7 at North Pond, a characteristic sediment-filled 70 km² depression surrounded by high relief
8 topography common to the western flank of the Mid-Atlantic Ridge (Becker et al.,
9 2001;Langseth et al., 1992). While a majority of seafloor subsurface biosphere research has
10 focused on aspects of sedimentary carbon, sulfur and iron cycles, the potential role of N in
11 supporting subsurface microbial activity has been largely unexplored. Despite exceedingly
12 oligotrophic conditions, life persists and evidence for active heterotrophic and autotrophic
13 microbial communities in North Pond sediments is mounting (Ziebis et al., 2012;Picard and
14 Ferdelman, 2011;Orcutt et al., 2013).

15 Nitrogen plays a central role as a limiting nutrient in many regions of the sunlit surface
16 ocean (Rabalais, 2002), as nearly 90% of the biologically available fixed N in the ocean resides
17 below the euphotic zone in the deep ocean NO₃⁻ reservoir (Gruber, 2008). Globally, sediments
18 (especially continental shelves) are considered a net sink of fixed nitrogen through reductive
19 anaerobic processes including denitrification and anaerobic ammonium oxidation (Christensen et
20 al., 1987;Devol, 1991;Prokopenko et al., 2013). For example, coupled nitrification (the
21 chemolithotrophic oxidation of NH₄⁺ to NO₃⁻) and denitrification (the typically heterotrophic
22 reduction of NO₃⁻ to N₂) have been shown to be important in N budgets in sediments of
23 continental shelves, ocean margins and estuaries (Risgaard-Petersen, 2003;Granger et al.,
24 2011;Lehmann et al., 2004;Lehmann et al., 2005;Wankel et al., 2009). There is abundant
25 evidence demonstrating the importance of both oxidative and reductive N cycling processes (and
26 their tight coupling) operating in sediment environments. In contrast to sediments on continental
27 shelves, however, data from sediments underlying large swaths of the oligotrophic ocean suggest
28 an entirely different framework. For example, NO₃⁻ concentration data from North Pond
29 demonstrate the accumulation of NO₃⁻ with depth (Ziebis et al., 2012) implicating the role of *in*
30 *situ* production supported by the autotrophic oxidation of ammonium and nitrite (e.g.,

1 nitrification). To what degree this NO_3^- pool supports other subsurface microbial communities as
2 an electron acceptor source, however, remains unclear. In addition, the supply of dissolved
3 substrates (O_2 , NO_3^- , DOC) from the underlying crustal aquifer may play a primary role in
4 supporting these deep sediment communities. At a global scale, this geochemical exchange
5 among crust, ocean and sediments across vast reaches of the seafloor, and its link to subsurface
6 microbial activity, may well be important for global biogeochemical cycles.

7 Dual isotopes of NO_3^- represent a powerful tool for disentangling the combined activities
8 of multiple N cycling processes (Casciotti et al., 2008; Lehmann et al., 2005; Sigman et al.,
9 2005; Wankel et al., 2007; Marconi et al., 2015; Fawcett et al., 2015). Nitrate-removal processes
10 (whether assimilatory or dissimilatory) have been shown to impart linearly coupled increases in
11 both N and O isotope ratios of the remaining NO_3^- pool (Karsh et al., 2012; Kritee et al.,
12 2012; Granger et al., 2008; Granger et al., 2004). In contrast, however, nitrification, the two-step
13 oxidation of NH_4^+ to NO_2^- followed by NO_2^- oxidation to NO_3^- , represents a decoupling of the N
14 and O isotope systems in the resulting nitrate (Casciotti and McIlvin, 2007; Buchwald and
15 Casciotti, 2013; Wankel et al., 2007). Whereas the N atoms derive from the NH_4^+ (which can be
16 assumed to originate from the sedimentary organic nitrogen pool), the oxygen atoms derive, to
17 varying degrees, from both water and dissolved O_2 (Buchwald and Casciotti, 2010; Buchwald et
18 al., 2012; Casciotti et al., 2010). Thus, by combining isotope mass balances of both N and O in
19 the NO_3^- system, along with our understanding of organism-level constraints on the isotope
20 systematics of these transformations, we can deduce the relative roles of multiple N cycling
21 processes (e.g., Wankel et al., 2009, Lehmann et al. 2004; Bourbonnais et al. 2009). Here we use
22 the dual isotopic composition of nitrate (N and O isotopes) as a record of microbial processes
23 occurring in the low-carbon sediments of North Pond underlying the oligotrophic North Atlantic
24 gyre. By combining the N and O isotope mass balance with an inverse reaction-diffusion model
25 approach, we use these data to estimate rates of nitrification and denitrification, and to provide
26 new constraints on some isotope parameters for these processes.

27 **2. MATERIAL AND METHODS**

28 **2.1 Sediment and porewater collection**

1 Sediment cores were collected at three sites in the North Pond Basin (Figure 1) as part of
2 the IODP Leg 336 expedition and have been described extensively elsewhere (Expedition-336-
3 Scientists, 2012a). Four boreholes were drilled (U1382B, U1383D, U1383E and U1384A,
4 referred to hereafter as ‘2B’, ‘3D’, ‘3E’ and ‘4A’). Sites 3D and 3E were next to each other and
5 as drilling logs indicated that the core from 3E showed excessive signs of disturbance upon
6 retrieval and potential contamination by seawater, it was excluded from our study. Sediment
7 cores were retrieved using the Advanced Piston Corer, which penetrated the seafloor sediments
8 until contact with basement, followed by extended core barrel coring of the upper section of
9 basement rock. Site 2B (~90m sediment thickness, depth to basement) is located in the deeper
10 part of the pond, approximately 25m away from DSDP ‘legacy hole’ 395A, which was
11 instrumented as a CORK observatory (Davis et al., 1992). Site 3D (~42m sediment thickness,
12 depth to basement) lies in the northeastern region towards the edge of North Pond (~5.9km away
13 from U1382A), whereas site 4A (~95m sediment thickness, depth to basement) is located on the
14 northwest side in a deeper part of the basin, approximately 3.9 and 6.2km distance from U1383
15 and U1382, respectively (Figure 1). Two decades of temperature and flow records revealed
16 vigorous subsurface flow (Becker et al., 1984; Gable et al., 1992), with geothermal surveys
17 indicating that recharge is from the southeastern side of the basin (near 2B and 3D) flowing to
18 the northwest (towards 4A) (Figure 1). All sediments were comprised of light-brown to brown
19 nanofossil ooze with intercalations of foraminiferal sand. In the lowest few meters close to the
20 sediment/basement contact, sediments exhibited a darker brown color and sometimes rust-
21 colored clay-rich zones (Edwards et al., 2012a; Expedition-336-Scientists, 2012b).

22 Porewater samples for concentration and stable isotope analyses were collected either
23 directly from cores on the shipboard catwalk immediately after core retrieval (and stored at -
24 80°C until analysis), from whole core rounds (~10cm core sections) that had been preserved at -
25 80°C for ~ 1 year until thawing and porewater extraction, or from subsampled sediments
26 collected shipboard and stored at -20°C for ~ 9 months. Porewaters from whole core rounds
27 (~40ml) and subsampled sediments (~3ml), were extracted using rhizon samplers (0.2µm)
28 (Seeberg-Elverfeldt et al., 2005) and stored frozen (-20°C) until analysis.

29 **2.2 Concentration measurements**

1 Concentrations of NO_x (i.e., NO_3^- plus NO_2^-) from shipboard-extracted porewaters were
2 measured via ion chromatography ~3 months after collection, while concentrations from home-
3 laboratory extracted porewaters were measured by chemiluminescence after reduction in a hot
4 acidic vanadyl sulfate solution on a NO_x analyzer (Braman and Hendrix, 1989) (detection limit
5 $<0.5\mu\text{M}$). Concentrations of NO_2^- were quantified by using the Griess-Ilosvay method followed
6 by measuring absorption at 540nm (Grasshoff et al., 2007) or by chemiluminescence in a sodium
7 iodide solution on a NO_x analyzer (Garside, 1982;Cox, 1980). NO_3^- was quantified by difference
8 between NO_x and NO_2^- (Grasshoff et al., 2007). Ammonium concentrations were measured using
9 the orthophthaldialdehyde fluorescence method with an empirically determined sensitivity limit
10 of $\sim 0.5\mu\text{M}$ for porewaters (Holmes et al., 1999).

11 **2.3 Nitrate stable isotope composition**

12 Nitrate N and O isotopic composition were measured using the denitrifier method
13 (Casciotti et al., 2002;Sigman et al., 2001), in which sample NO_3^- is quantitatively converted to
14 N_2O using a lab-grown denitrifying bacterium before being extracted and purified on a purge-
15 and-trap system similar to that previously described (McIlvin and Casciotti, 2010). Where
16 detected (O_2 -depleted zones of 2B), NO_2^- was removed by sulfamic acid addition (Granger and
17 Sigman, 2009) prior to isotopic analysis of the NO_3^- . Isotopic analysis of shipboard extracted
18 samples (16) were conducted at the University of Basel using a Delta V Advantage (Thermo,
19 Inc.), while all other samples (29) were measured on an IsoPrime100 (Elementar, Inc.).
20 Corrections for drift, size and fractionation of O isotopes during bacterial conversion were
21 carried out as previously described using NO_3^- standards USGS 32, USGS 34 and USGS 35
22 (Casciotti et al., 2002;McIlvin and Casciotti, 2011), with a typical reproducibility of 0.2‰ and
23 0.4‰ for $\delta^{15}\text{N}$ and $\delta^{18}\text{O}$, respectively.

24 **3. RESULTS**

25 **3.1 Previous measurements of dissolved oxygen and organic matter content at North Pond**

26 Oxygen penetration depths, which have been discussed previously (Orcutt et al., 2013),
27 vary distinctly among the three sites at North Pond indicating much greater respiratory
28 consumption in 2B than in the profiles of other two sites, 3D and 4A (Figure 2). In 2B, dissolved
29 oxygen levels are drawn down to near detection by a depth of about 10mbsf (although low levels

1 of dissolved O₂ seem to persist as deep as 30mbsf). In contrast, at site 3D, dissolved O₂ levels are
2 drawn down close to the detection limit (~5μM) for an interval of only ~3m between a depth of
3 ~30 to ~33mbsf and in 4A, zero-level O₂ concentrations were observed over the interval between
4 32 and 54m. At North Pond, O₂ (and NO₃⁻) is also supplied via diffusion from the underlying
5 basaltic crustal aquifer (Figure 2) (Orcutt et al., 2013; Ziebis et al., 2012). Although not measured
6 during this work, sediment organic carbon and nitrogen content was measured on several of the
7 piston cores collected during the site-survey, averaging 0.15% and 0.02%, respectively (Ziebis et
8 al., 2012). Although quantification of such low organic-N and -C levels is challenging and is
9 afflicted with relatively large uncertainties, no discernable OM-elemental differences among the
10 sites were noted (Ziebis et al., 2012). Similarly, no differences in organic phosphorus content
11 were noted among the three sites (Defforey and Paytan, 2015).

12 **3.2 NO₃⁻ and NO₂⁻ concentration profiles**

13 Bottom seawater NO₃⁻ concentration at North Pond is approximately 21.6μM (Ziebis et
14 al., 2012). At all depths in all three profiles, porewater NO₃⁻ concentrations exceeded bottom
15 water NO₃⁻ concentrations, reflecting the production of NO₃⁻ by nitrification and the net flux of
16 NO₃⁻ to the overlying water from this site of ~4.6 μmoles m⁻² d⁻¹ (Ziebis et al., 2012), consistent
17 with other studies of NO₃⁻ fluxes in pelagic deep-sea sediments (Berelson et al., 1990; Goloway
18 and Bender, 1982; Hammond et al., 1996; Jahnke et al., 1982; Grundmanis and Murray, 1982).
19 More precisely, below the sediment-water interface, NO₃⁻ concentrations increased significantly
20 with depth (Figure 2), before decreasing again with proximity to the basement/sediment contact.
21 Mid-profile NO₃⁻ concentration maxima reached 38.2, 42.2 and 49.1μM at depths of 19.1, 23.0
22 and 56.3mbsf in the cores from sites 2B, 3D and 4A, respectively, - depths that generally
23 coincided with O₂ concentrations below 10μM. Nitrite was below detection at sites 3D and 4A
24 and was only detected at anoxic depths in site 2B (Figure 2), where concentrations of up to 6.0
25 and 6.6 μM were observed at depths of 36 and 59m, respectively.

26 **3.3 NO₃⁻ N and O isotopic composition**

27 Down-core changes in δ¹⁵N and δ¹⁸O varied markedly among the three cores (Figure 2).
28 The most prominent changes in both δ¹⁵N and δ¹⁸O were observed at site 2B (which had the
29 most extensive O₂ depleted zone), in which δ¹⁵N increased with depth from a value of +5.4‰

1 (bottom seawater) to a maximum of +23.3‰ at a depth of 59.2 mbsf and $\delta^{18}\text{O}$ increased from a
2 bottom seawater value of +1.8‰ to a maximum of +23.8‰ at a much shallower depth of 32.1
3 mbsf. Isotopic maxima generally coincided with depths of lowest O_2 concentrations, except in
4 3D, where the maximum was observed at slightly greater depth than the O_2 minimum (Figure 2).
5 Substantial N and O isotopic shifts were also observed at site 3D, in which increases above
6 bottom water NO_3^- values to $\delta^{15}\text{N}$ of +11.8‰ and a $\delta^{18}\text{O}$ of +21.7‰ were observed, with both
7 maxima occurring at a depth of 37mbsf. In contrast, site 4A exhibited only very modest changes
8 relative to bottom seawater, with a maximum $\delta^{15}\text{N}$ value of +7.0‰ at a depth of 38.8 mbsf and a
9 maximum $\delta^{18}\text{O}$ value of +6.3‰ at a depth of 44.1 mbsf. Strong correlations were also observed
10 between $\delta^{15}\text{N}_{\text{NO}_3^-}$ and $\delta^{18}\text{O}_{\text{NO}_3^-}$ (Figure 3), with $\delta^{18}\text{O}_{\text{NO}_3^-}$ values always increasing more than the
11 corresponding $\delta^{15}\text{N}_{\text{NO}_3^-}$. The relationship between $\delta^{18}\text{O}_{\text{NO}_3^-}$ and $\delta^{15}\text{N}_{\text{NO}_3^-}$ exhibited a slope of 1.8
12 for the upper portion of the 2B profile, 3.0 for the 3D profile and 2.4 for the 4A profile –
13 consistently exceeding the 1:1 relationship expected from NO_3^- consumption alone. In 2B,
14 sampling points near the most O_2 depleted depths and the lower portion of the profile fell closer
15 to the expected 1:1 line for NO_3^- consumption by denitrification (Figure 3).

16 **4. DISCUSSION**

17 The distribution of porewater nitrate in deep-sea sediments is controlled by the combined
18 influence of diffusion as well as several biologically catalyzed diagenetic processes including
19 nitrification (ammonia and nitrite oxidation to nitrate) and denitrification (loss of N via nitrate
20 reduction to gaseous products, NO , N_2O or N_2). Here we use the concentration and dual N and O
21 stable isotope composition of porewater NO_3^- to gain insight into the magnitude and distribution
22 of N transformation processes. In comparison to models that predict the rates of these processes
23 based solely on concentration profiles of NO_3^- and O_2 , for example, our approach estimates rates
24 using the added constraints provided by recent studies of N and O isotope systematics of
25 nitrification and denitrification (Granger et al., 2008;Buchwald and Casciotti, 2010;Casciotti et
26 al., 2010;Buchwald et al., 2012). In particular, while there are strong and related N and O isotope
27 effects during denitrification (Granger et al., 2008), the isotopic transformations of N and O are
28 decoupled due to differently sourced N and O atoms during nitrate production (Buchwald and
29 Casciotti, 2010;Casciotti et al., 2010;Buchwald et al., 2012). Thus, changes in N and O isotopic
30 composition between intervals of any one depth are the combined result of both diffusion of

1 NO_3^- to/from overlying (and underlying) seawater, together with microbially mediated
2 production and/or consumption of NO_3^- within porewaters. Under low oxygen, NO_3^- respiration
3 by denitrification leads to a well-characterized increase in both $\delta^{15}\text{N}$ and $\delta^{18}\text{O}$ in conjunction
4 with decreasing NO_3^- concentrations. In contrast, nitrification produces NO_3^- with a $\delta^{15}\text{N}$ equal
5 to the starting NH_4^+ (when accumulation of NH_4^+ and NO_2^- is negligible), while the $\delta^{18}\text{O}$ of the
6 newly produced NO_3^- is set by the $\delta^{18}\text{O}$ of ambient H_2O and O_2 , as well as kinetic and
7 equilibrium isotope effects associated with the stepwise oxidation of NH_4^+ to NO_3^- . While
8 elevated NO_3^- concentrations indicate nitrification, extensive zones of low O_2 (and NO_3^- replete)
9 porewaters also suggest a high potential for denitrification, which can be verified using nitrate
10 dual isotope measurements. In this way, our modeling approach provides an assessment of the
11 distribution of these N transformations, as well as some additional insights on the nature of N
12 and O source atoms to NO_3^- in these energy-lean systems. Specifically, we show below that the
13 profiles of $\delta^{15}\text{N}_{\text{NO}_3}$ and $\delta^{18}\text{O}_{\text{NO}_3}$ can be explained by variations in the magnitude of nitrification
14 and denitrification occurring throughout the sediment column, including substantial zones of
15 overlap of these aerobic/anaerobic processes. Finally, we use our model to predict the $\delta^{18}\text{O}$ and
16 $\delta^{15}\text{N}$ stemming from nitrate production by nitrification, offering insights into both the nature of
17 processes setting the O isotopic composition of oceanic NO_3^- , as well as the sources of N and/or
18 the isotopic partitioning of available N sources in global ocean sediments.

19 **4.1 Diffusion-Reaction Model**

20 The diffusion-reaction inverse modeling approach used here is conceptually similar to
21 other early diagenetic models that simulate porewater profiles of dissolved species through a
22 sediment column harboring both oxic and anoxic organic matter remineralization (Christensen
23 and Rowe, 1984; Goloway and Bender, 1982; Jahnke et al., 1982). It is an inverse modeling
24 approach adapted to distinguish between heavy and light nitrate isotopologues (e.g., (Lehmann et
25 al., 2007)). Specifically, we use the model to estimate rates of nitrification and denitrification
26 required to fit the concentration profiles of each isotopologue, $^{14}\text{N}^{16}\text{O}_3^-$, $^{15}\text{N}^{16}\text{O}_3^-$, and
27 $^{14}\text{N}^{18}\text{O}^{16}\text{O}_2^-$ (and, thus, $\delta^{15}\text{N}_{\text{NO}_3}$ and $\delta^{18}\text{O}_{\text{NO}_3}$ values) under the assumption of steady-state
28 diffusion and microbial production (by nitrification) and/or consumption (by denitrification).
29 Rates of nitrification and denitrification in each porewater sampling interval (e.g., defined as the
30 distance between the lower and upper midpoints between sampling depths) were estimated

1 numerically by least squares fitting of the system of equations describing the distribution of each
 2 isotopologue (using a genetic algorithm included in the Solver package of Microsoft Excel 2011).
 3 This approach involves determination of a non-unique solution using numerical iteration and
 4 optimization, and is repeatedly iterated to evaluate robustness of model fits. Certain parameters
 5 are allowed to be optimizable by the model, including both the magnitude of, and connection
 6 between, the N and O isotope effects for denitrification ($^{15}\epsilon_{DNF}$ and $^{18}\epsilon_{DNF}$; $^{15}\epsilon_{DNF}$, respectively),
 7 as well as the N and O isotopic composition of new NO_3^- produced by nitrification ($\delta^{15}\text{N}_{NTR}$ and
 8 $\delta^{18}\text{O}_{NTR}$, respectively). Uncertainty in model-estimates is expressed as the standard error of 10
 9 model-run estimates (Table 1). Conditions at the uppermost part of the sediment column were
 10 constrained by measured concentrations and isotope ratios in bottom seawater. Measured
 11 concentrations of the NO_3^- isotopologues within each interval, together with the diffusive fluxes
 12 defined by the concentration gradients between the over/underlying intervals, were used for
 13 model fitting by least-squares optimization of microbial rates of nitrification and/or
 14 denitrification.

15 As measurable NH_4^+ was not observed at any depths, it is not included in the model. NO_3^-
 16 is the only dissolved N species included in the model and we assume that all NH_4^+ generated by
 17 remineralization is completely oxidized to NO_3^- (see below). To minimize complexity, other
 18 diagenetic reactions that may be important in many sedimentary environments, including
 19 anaerobic NH_4^+ oxidation, removal of N species through interactions with Fe or Mn and the
 20 adsorption and retention of NH_4^+ by clay minerals are not specifically addressed. We also
 21 neglect effects of compaction as well as potential changes in organic matter reactivity with depth.
 22 No difference in the diffusivity among NO_3^- isotopologues was included, since these differences
 23 are considered to be very small (Clark and Fritz, 1997).

24 Resolving the vertical dimension only, the mass balance differential equations are as follows:

$$25 \quad \frac{\partial C_{14NO3}}{\partial t} = \frac{\partial}{\partial z} \left(D_{NO3} \frac{\partial C_{14NO3}}{\partial z} \right) - DNF_{14N} + NTR_{14N} \quad (1)$$

$$26 \quad \frac{\partial C_{15NO3}}{\partial t} = \frac{\partial}{\partial z} \left(D_{NO3} \frac{\partial C_{15NO3}}{\partial z} \right) - DNF_{15N} + NTR_{15N} \quad (2)$$

$$27 \quad \frac{\partial C_{16NO3}}{\partial t} = \frac{\partial}{\partial z} \left(D_{NO3} \frac{\partial C_{16NO3}}{\partial z} \right) - DNF_{16O} + NTR_{16O} \quad (3)$$

$$1 \quad \frac{\partial C_{18NO_3}}{\partial t} = \frac{\partial}{\partial z} \left(D_{NO_3} \frac{\partial C_{18NO_3}}{\partial z} \right) - DNF_{18O} + NTR_{18O} \quad (4)$$

2 such that for denitrification (DNF):

$$3 \quad DNF_{14N} = C_{14NO_3} * k_{DNF} \quad (5a)$$

$$4 \quad DNF_{15N} = C_{15NO_3} * k_{DNF} / \alpha_{DNF} \quad (5b)$$

$$5 \quad DNF_{16O} = C_{16NO_3} * k_{DNF} \quad (5c)$$

$$6 \quad DNF_{18O} = C_{18NO_3} * k_{DNF} / [1 + ((\alpha_{DNF} - 1) * ({}^{18}\epsilon : {}^{15}\epsilon_{DNF}))] \quad (5d)$$

$$7 \quad DNF = DNF_{14N} + DNF_{15N} = DNF_{16O} + DNF_{18O} \quad (6)$$

8 where D refers to the molecular diffusion coefficient for NO_3^- adjusted for porosity, DNF and
9 NTR refers to the reaction rate of denitrification or nitrification, respectively (in mass volume⁻¹
10 time⁻¹), C refers to the concentration of each isotopologue (in mass volume⁻¹) and k refers to the
11 first order rate constant (time⁻¹). The fractionation factor, α , is defined as the ratio of rate
12 constants for the light isotope over the heavy isotope (e.g., ${}^{15}\alpha = {}^{14}k / {}^{15}k$) for a given process,
13 alternatively expressed in terms of epsilon where $\epsilon = (\alpha - 1) * 1000$ in units of permil (‰). The
14 term ${}^{18}\epsilon : {}^{15}\epsilon_{DNF}$ refers to the degree of coupling between the N and O isotope fractionation during
15 denitrification, with a value of 1 indicating that the two isotope effects are identical.

16 For the $\delta^{15}N$ and $\delta^{18}O$ of nitrification (NTR)

$$17 \quad NTR_{14N} = NTR * f_{14NNTR} \quad (7a)$$

$$18 \quad NTR_{15N} = NTR * f_{15NNTR} \quad (7b)$$

$$19 \quad NTR_{16O} = NTR * f_{16ONTR} \quad (7c)$$

$$20 \quad NTR_{18O} = NTR * f_{18ONTR} \quad (7d)$$

21 where f refers to the fractional abundance of a particular isotopologue and

$$22 \quad NTR = NTR_{14N} + NTR_{15N} = NTR_{16O} + NTR_{18O} \quad (8)$$

$$23 \quad f_{14NNTR} = 1 / (1 + {}^{15}R_{NTR}) \quad (9a)$$

1 $f_{15\text{NNTR}} = 1 - f_{14\text{NNTR}}$ (9b)

2 $^{15}\text{R}_{\text{NTR}} = [^{15}\text{N}/^{14}\text{N}]_{\text{NTR}}$ (9c)

3 and

4 $f_{16\text{ONTR}} = 1/(1+^{18}\text{R}_{\text{NTR}})$ (10a)

5 $f_{18\text{ONTR}} = 1 - f_{16\text{ONTR}}$ (10b)

6 $^{18}\text{R}_{\text{NTR}} = [^{18}\text{O}/^{16}\text{O}]_{\text{NTR}}$ (10c)

7 and $^{15}\text{R}_{\text{NTR}}$ and $^{18}\text{R}_{\text{NTR}}$ are used to calculate the $\delta^{15}\text{N}_{\text{NTR}}$ and $\delta^{18}\text{O}_{\text{NTR}}$, respectively.

8 For parameterizing diffusion, we use a porewater diffusion coefficient (D_s) based on the
 9 molecular diffusion coefficient (D_m at 5 °C) for NO_3^- of $1.05 \cdot 10^{-5} \text{ cm}^2 \text{ s}^{-1}$ (Li and Gregory,
 10 1974) adjusted for an average porosity (ϕ) of North Pond sediments of 64% (Expedition-336-
 11 Scientists, 2012a), where $D_s = \phi^k D_m$ and k is an empirically derived factor (we use 2.6)
 12 accounting for tortuosity of pore space (Hammond et al., 1996;McManus et al., 1995).

13 Compared with contemporaneous profiles of O_2 and Sr (Orcutt et al., 2013) and other
 14 dissolved ions, the NO_3^- concentration profiles suffer from some apparent analytical noise. The
 15 nature of the heterogeneity for NO_3^- concentration measurements was unclear. However, it is
 16 unlikely that this heterogeneity is environmental and we attribute it to small amounts of
 17 evaporation during freezer storage of the sediments, which is supported by the apparent
 18 smoothness of the isotopic measurements (evaporation would change the apparent concentrations
 19 without influencing the isotopic composition of solutes such as NO_3^-). As such, for the purpose
 20 of the diffusion-reaction model, we applied a 5-point weighted triangular smoothing to the
 21 concentration data to eliminate outliers and unrealistically sharp gradients (Figure 2). Given the
 22 relatively smooth and contiguous vertical profiles of $\delta^{15}\text{N}_{\text{NO}_3}$ and $\delta^{18}\text{O}_{\text{NO}_3}$, only very minor
 23 smoothing to these data was required using a similar approach (Figure 2).

24 Within this model architecture, we explore the influence of four key parameters that
 25 could affect the estimation of nitrification and denitrification rates by this isotope mass balance
 26 approach, specifically, $^{15}\epsilon_{\text{DNF}}$, $^{18}\epsilon$, $^{15}\epsilon_{\text{DNF}}$, $\delta^{15}\text{N}_{\text{NTR}}$ and $\delta^{18}\text{O}_{\text{NTR}}$. Specifically, the expression of the

1 full enzymatic level isotope effect ($^{15}\epsilon_{\text{DNF}}$) for denitrification (27‰) can be influenced by
2 electron donor, carbon substrate quality, denitrification rate and metabolic activity (Kritee et al.,
3 2012). Moreover, although the relationship between the kinetic isotope effects for ^{18}O and ^{15}N
4 during respiratory consumption of NO_3^- by denitrification (e.g., $^{18}\epsilon:^{15}\epsilon_{\text{DNF}}$) has been shown to
5 remain consistent at 1:1, the potential influence of nitrate reduction by periplasmic nitrate
6 reductase (Nap), which imparts a lower $^{18}\epsilon:^{15}\epsilon_{\text{DNF}}$ value of 0.6 (Granger et al., 2008; Frey et al.,
7 2014), could play a role in the dual isotope trajectory of NO_3^- consumption (Wenk et al., 2014).
8 Further, in the absence of NH_4^+ accumulation in these sediments, the $\delta^{15}\text{N}_{\text{NTR}}$ is equal to the
9 source of NH_4^+ being oxidized to NO_3^- , which is related to the $\delta^{15}\text{N}$ of the organic matter being
10 remineralized. The $\delta^{18}\text{O}_{\text{NTR}}$ stems from a combination of factors including the $\delta^{18}\text{O}$ of the water
11 and dissolved O_2 as well as the expression of kinetic isotope effects associated with the
12 incorporation of O atoms from these pools (Buchwald and Casciotti, 2010; Casciotti et al.,
13 2010; Andersson and Hooper, 1983). Below, we use the model to optimize and predict these
14 values and to explore the sensitivity of rate estimates to $^{15}\epsilon_{\text{DNF}}$.

15 The model contains more parameters than can be explicitly estimated from the small
16 number of data points measured. To minimize the number of variables as much as possible (and
17 maximize the utility of the approach for constraining other variables), we adapt the model
18 implementation for three different O_2 regimes: 1) ‘oxic intervals’ where O_2 is poised as the more
19 energy-yielding oxidant with respect to NO_3^- (here generally $\text{O}_2 > \sim 40\mu\text{M}$) and in which only
20 nitrification is allowed to occur, 2) ‘transitional intervals’ in which both denitrification and
21 nitrification may occur (O_2 between $\sim 40\mu\text{M}$ and $2\mu\text{M}$) and 3) ‘anoxic intervals’ where O_2 is
22 $< 2\mu\text{M}$ and in which only denitrification is allowed to occur. We choose $40\mu\text{M}$ as a boundary for
23 the onset of denitrification based on estimates of thermodynamic energy yield under these
24 conditions for aerobic vs denitrification-based respiration (Brewer et al., 2014). In the oxic
25 intervals – the model is used for parameter estimation of both $\delta^{15}\text{N}_{\text{NTR}}$ and $\delta^{18}\text{O}_{\text{NTR}}$ (in addition
26 to nitrification rate), while in the anoxic intervals the model is used to estimate $^{15}\epsilon_{\text{DNF}}$ and
27 $^{18}\epsilon:^{15}\epsilon_{\text{DNF}}$ (in addition to denitrification rate). In transitional intervals, $^{15}\epsilon_{\text{DNF}}$ and $^{18}\epsilon:^{15}\epsilon_{\text{DNF}}$ are
28 held constant at 25‰ and 1, respectively, and the parameter $\delta^{15}\text{N}_{\text{NTR}}$ and $\delta^{18}\text{O}_{\text{NTR}}$ are estimated
29 through model fitting, together with rates of both nitrification and denitrification. In accordance
30 with previous experimental work (Buchwald and Casciotti, 2010; Buchwald et al., 2012; Casciotti

1 et al., 2010), the allowed range of values for $\delta^{15}\text{N}_{\text{NTR}}$ and $\delta^{18}\text{O}_{\text{NTR}}$ were set to -5 to +10‰ and -5
2 to +20‰, respectively. When $^{15}\epsilon_{\text{DNF}}$ and $^{18}\epsilon_{\text{DNF}}$ were determined by model fitting, parameter
3 estimates were allowed to range between 0 and 30‰ and between 0.6 and 1.2, respectively.

4

5 **4.2 Model Results and Implications**

6 ***4.2.1 Model Estimated Rates of Nitrification and Denitrification***

7 Profiles of sedimentary porewater solutes reflect the combined influence of many
8 processes including diagenetic reactions, which are intimately related to the availability,
9 abundance and quality of organic carbon. In particular, the distribution of dissolved substrates
10 that are available as electron acceptors for microbial respiration of organic carbon, generally
11 reflect stepwise consumption by the most thermodynamically (and kinetically) favorable
12 metabolic processes (e.g., O_2 consumption precedes NO_3^- consumption, which precedes sulfate
13 reduction, etc.). While in organic rich estuarine and continental shelf sediments, dissolved O_2
14 and NO_3^- are typically consumed within a few cm or mm below the sediment-seawater interface,
15 sediments underlying large areas of the oligotrophic ocean are characterized by very deep
16 penetration of O_2 , in some cases even penetrating to the underlying ocean crust (D'Hondt et al.,
17 2015;D'Hondt et al., 2009;Orcutt et al., 2013;Ziebis et al., 2012). In connection with this deep
18 penetration of O_2 , deep-sea sediment porewaters also often exhibit extensive accumulation of
19 NO_3^- above ambient seawater concentrations, associated with the oxidation of NH_4^+ released by
20 aerobic remineralization of sediment organic matter (and linked to the consumption of O_2
21 through Redfield stoichiometry) (Berelson et al., 1990;Christensen and Rowe, 1984;D'Hondt et
22 al., 2009;Goloway and Bender, 1982;Seitzinger et al., 1984). In organic-rich sediments, NO_3^-
23 concentration profiles may exhibit maxima only a few mm or cm below the sediment/water
24 interface. In contrast, in the deep-sea sediments underlying the oligotrophic regions of the ocean,
25 the sedimentary zone where NO_3^- accumulates to 10 to 30 μM above bottom seawater
26 concentrations can extend over a much larger vertical extent and nitrate maxima can be found
27 tens of meters below the seafloor. In effect, the redox zonation of O_2 respiration, NH_4^+ oxidation,
28 NO_2^- oxidation and NO_3^- reduction extends over larger depth ranges, and, depending on sediment

1 thickness and organic carbon content – the redox state of these sediments may never reach the
2 potential for NO_3^- reduction to play a role as a thermodynamically viable metabolic pathway.

3 While it is not necessarily apparent whether any NO_3^- respiration is occurring based on
4 North Pond concentration profiles alone, dramatic increases in the $\delta^{15}\text{N}$ and $\delta^{18}\text{O}$ of NO_3^- with
5 depth into the anoxic sediment intervals were observed in both 2B and 3D (Figure 2) – indicating
6 isotope fractionation by microbial denitrification. The highest $\delta^{15}\text{N}$ and $\delta^{18}\text{O}$ values in 2B
7 (+22.2‰ and +21.8‰, respectively) generally coincide with the lowest dissolved O_2 , while
8 highest $\delta^{15}\text{N}$ and $\delta^{18}\text{O}$ values in 3D (+11.8‰ and + 19.7‰, respectively) fall just below the
9 depth of lowest O_2 . In stark contrast, 4A porewaters exhibit only a minor increase in $\delta^{18}\text{O}$ of
10 $\sim 2.7\%$ within the anoxic interval, while $\delta^{15}\text{N}$ increased by only 0.8‰ (Figure 2). The marked
11 distinction between 2B/3D and 4A notwithstanding, the dual isotopic composition and
12 concentrations of NO_3^- in these porewaters reveal active nitrogen cycling within all three sites.

13 Using these changes in dual NO_3^- isotopic composition and concentration, we calculated
14 the rates of nitrification and denitrification necessary to produce the observed patterns within
15 each interval (in the transitional intervals, here we prescribe a value of 25‰ for $^{15}\epsilon_{\text{DNF}}$, but
16 explore the model sensitivity to this value later). Rates of nitrification and denitrification varied
17 with depth, as well as across the three sites (Figure 4; Table 1). Estimated rates of nitrification in
18 the oxic and transitional intervals were up to $871 \text{ nmol cm}^{-3} \text{ yr}^{-1}$, while rates of denitrification in
19 the anoxic and transitional intervals reached up to $579 \text{ nmol cm}^{-3} \text{ yr}^{-1}$ (Figure 4; Table 1). By
20 comparison, maximum rates of nitrification estimated from O_2 and NO_3^- profiles in sediments
21 below the South Pacific Gyre, perhaps the most organic matter depleted seafloor sediments in the
22 world, were predicted to be only as high as $18 - 74 \text{ nmol cm}^{-3} \text{ yr}^{-1}$ (D'Hondt et al., 2009). The
23 estimated nitrification rates at North Pond are still orders of magnitude lower than those typically
24 measured in coastal and estuarine sediments (Rysgaard et al., 1993; Usui et al., 2001; Wankel et
25 al., 2011), and are, thus, consistent with lower total cell abundances and lower abundance of
26 functional genes involved in nitrification recently measured in North Pond sediments (Zhao and
27 Jørgensen, in review) as compared to typical estuarine sediments (Mosier and Francis,
28 2008; Wankel et al., 2011).

1 In general, nitrification rates in the oxic intervals near the seafloor were comparable to
2 rates in the oxic layers near the underlying crust. The highest denitrification rates typically
3 coincided with depths where lowest O₂ were observed, with the exception of rather low rates
4 near the central anoxic zone of core 2B. Nitrification, which requires O₂, is observed as deep as
5 28m in 2B and all the way to the underlying crust at the other two sites. Interestingly, modeled
6 rates of nitrification were typically highest at comparatively low levels of dissolved O₂ (~15μM
7 in 2B, ~10μM in 3D and ~35μM in 4A) – suggesting an important role for micro-aerophilic
8 nitrification (e.g., organisms adapted to respiration under low O₂ conditions). The depths of
9 maximum denitrification rates generally coincided with the onset of O₂ levels below ~2μM. In
10 2B, denitrification rates were highest at depths of ~28m and ~72m (Figure 4). In 3D, maximum
11 denitrification rates were observed at 21m – with similar rates between 20 and 25m. Interestingly,
12 the model indicated no denitrification within the 3m anoxic zone of this core – possibly
13 indicating limitation by organic substrate availability. In contrast, rates of denitrification were
14 only estimated to occur within the anoxic zone of site 4A (e.g., not within the transitional
15 intervals, although this was somewhat sensitive to prescribed ¹⁵ε_{DNF}, see below), with the highest
16 rate of 24 nmol cm⁻³ yr⁻¹ at a depth of 44m. Overall, rates of both nitrification and denitrification
17 were highest at site 2B and lowest in 4A, consistent with a greater amount of microbial activity
18 revealed by the steeper O₂ gradients in 2B and recent functional gene quantification in NP
19 sediments (Zhao and Jørgensen, in review). More precisely, the abundance of 16S rRNA, and
20 several functional genes, including those for both archaeal and bacterial ammonia oxidation,
21 nitrite oxidation, and denitrification, were all significantly lower in 4A than in the other cores
22 (Zhao and Jørgensen, in review). In all three cores, maximum rates of nitrification exceeded
23 those of denitrification, consistent with the net accumulation of NO₃⁻ throughout the sediment
24 column. Even in 2B, where O₂ is below 2μM over an interval of ~40m, the NO₃⁻ concentration
25 profile exhibits no obvious influence by NO₃⁻ reduction (Figure 2).

26 Finally, the model suggests the co-occurrence of nitrification and denitrification (Figure
27 4) in the transition zones of our model (depths at which O₂ is between 2 and 40 μM). Although
28 denitrification rates generally did not exceed those of nitrification where the two processes are
29 co-occurring (i.e., no net nitrate consumption), the increasing δ¹⁵N and δ¹⁸O of NO₃⁻ clearly
30 reflects the influence of NO₃⁻ loss via denitrification. Indeed, similar inferences have also been

1 made about such overlap of nitrification and denitrification albeit in the much deeper and
2 organic-rich hadopelagic sediments of the Ogasawara Trench (Nunoura et al., 2013). This
3 observation illustrates the exceptionally extended vertical redox zonation of these sediments –
4 and highlights the potential interaction between nitrogen transformations that are classically
5 considered spatially explicit.

6 ***4.2.2 Model-predicted values of $\delta^{15}\text{N}_{\text{NTR}}$: Implications for N sources and processes in*** 7 ***oligotrophic sediments***

8 In general, where NH_4^+ from remineralization does not accumulate, it is expected that the
9 $\delta^{15}\text{N}$ of NO_3^- produced by NH_4^+ oxidation will be equivalent to the $\delta^{15}\text{N}$ of the NH_4^+ deriving
10 from remineralization of organic nitrogen. The $\delta^{15}\text{N}$ of organic N of the North Pond sediments
11 was not quantified in this study (N content as measured by Ziebis et al. (2012) within the upper
12 8m was <0.03%). Yet, the average model-predicted $\delta^{15}\text{N}$ of newly produced NO_3^- ($\delta^{15}\text{N}_{\text{NTR}}$)
13 (Figure 5) ranged from -3.1 to +1.1‰ (standard error typically ± 0.3 to 0.4‰), generally lower
14 than that expected based on the $\delta^{15}\text{N}$ of sinking organic matter from the surface ocean of
15 $\sim +3.7\%$ (Altabet, 1988; Altabet, 1989; Knapp et al., 2005; Ren et al., 2012). Values of $\delta^{15}\text{N}_{\text{NTR}} >$
16 +1‰ were only observed just above the O_2 minimum at sites 2B and 3D (Figure 5).

17 Confronted with this difference, we turn to other factors that might play a role in setting
18 the $\delta^{15}\text{N}_{\text{NTR}}$. The lower $\delta^{15}\text{N}$ values of newly produced NO_3^- can potentially be explained by a
19 number of possible processes including: 1) isotopic fractionation during remineralization, 2)
20 competitive branching between NH_4^+ oxidation (whether anaerobic or aerobic) and NH_4^+
21 assimilation or 3) contribution of low $\delta^{15}\text{N}$ through organic matter derived from sedimentary N_2
22 fixation.

23 Nitrogen isotope fractionation during organic matter remineralization has been reported
24 (Altabet, 1988; Altabet et al., 1999; Estep and Macko, 1984; Lehmann et al., 2002), whereby the
25 preferential remineralization of low $\delta^{15}\text{N}$ organic matter leads to production of low $\delta^{15}\text{N}$ NH_4^+
26 (which could feed into the production of low $\delta^{15}\text{N}$ NO_3^-). The influence of this phenomenon is
27 more likely, however, during remineralization of fresh organic matter and where the
28 heterotrophic community has abundant access to highly labile proteinaceous organic matter

1 (Altabet, 1988; Estep and Macko, 1984). At North Pond, given the extremely low levels of
2 organic material present in the sediments, it seems unlikely that preferential utilization of low
3 $\delta^{15}\text{N}$ organic material during diagenesis is responsible for the low $\delta^{15}\text{N}_{\text{NTR}}$.

4 Competitive branching of NH_4^+ supporting simultaneous nutritional supply (as an N
5 source) and energy supply (via autotrophic ammonia oxidation) has been used to explain NO_3^-
6 dual isotopic signatures in N-rich surface waters (Wankel et al., 2007). Because N isotope
7 fractionation during ammonia oxidation is generally thought to be stronger than that of NH_4^+
8 assimilation by phytoplankton under surface-water conditions, it was argued that this competitive
9 branching can lead to a shunt of low $\delta^{15}\text{N}$ into the NO_3^- pool via ammonia oxidation (Wankel et
10 al., 2007). In contrast to the high-nutrient, sunlit, productive waters of Monterey Bay, however,
11 under the energy-limited, and extremely low- NH_4^+ -production conditions in North Pond
12 porewaters, it is not clear whether the same mechanisms of NH_4^+ partitioning are operating.

13 Although North Pond porewaters contain abundant NO_3^- , assimilation of NO_3^- as a
14 nutritional N source requires an associated metabolic energy for reduction of NO_3^- (via an
15 assimilatory nitrate reductase), a costly process in this energy poor environment. On the other
16 hand, although NH_4^+ is more easily assimilated by most microbes, its exceedingly low
17 abundance (<20nM) in North Pond porewaters reflect its scarcity as a source of N required for
18 cell growth. Based on the estimated values of the N isotope effect for NO_3^- consumption (by
19 denitrification) in the porewaters of 2B that average ~20‰ (Table 2), there is little suggestion of
20 NO_3^- assimilation, which would lead to much lower estimated values of $^{15}\epsilon_{\text{DNF}}$ (Granger et al.,
21 2010). Thus, it is more likely that nutritional N originates from a reduced form such as NH_4^+
22 and/or organic N. If the N isotope effect for ammonia oxidation is much larger than that of
23 ammonia assimilation, then such a competitive branching effect may also be contributing to a
24 low $\delta^{15}\text{N}_{\text{NTR}}$. Although under such low concentrations, it is likely that microbial acquisition of
25 NH_4^+ (whether for assimilation or for oxidation) is diffusion-limited, conditions under which the
26 N isotope effect is expected to be near 0‰ (Hoch et al., 1992), a strong difference in the isotope
27 effects for assimilation and oxidation of NH_4^+ could still contribute to the production of low $\delta^{15}\text{N}$
28 nitrate.

1 A final possibility for the low values of $\delta^{15}\text{N}_{\text{NTR}}$ could reflect the relative importance of
2 benthic N_2 fixation operating in North Pond sediments. Bacterial N_2 fixation is generally thought
3 to result in biomass having a $\delta^{15}\text{N}$ between -2 and 0‰ (Delwiche et al., 1979; Meador et al.,
4 2007; Minigawa and Wada, 1986), which could effectively introduce new N and decrease the
5 bulk $\delta^{15}\text{N}$ available for oxidation. Benthic N_2 fixation is not generally considered to be an
6 important enough contributor to the total sediment organic matter to influence the bulk $\delta^{15}\text{N}$
7 values of sediment organic matter. However, given the low organic matter flux to these
8 sediments from the overlying oligotrophic surface waters, a proportionately smaller amount of
9 N_2 fixation would be required to significantly impact the sediment organic $\delta^{15}\text{N}$ value. While N_2
10 fixation is an energetically costly metabolism and might seem an unlikely strategy given the
11 abundant porewater NO_3^- pool, it has been recently acknowledged that N_2 fixation in benthic
12 environments may be widely underestimated, despite high levels of porewater DIN including
13 NO_3^- and/or NH_4^+ (Knapp, 2012).

14 In fact, N_2 fixation could be ecologically favored in organic-lean sediments like those at
15 North Pond owing to the formation of H_2 as an end product, which might afford some
16 community level. Although primarily recycled by highly efficient hydrogenases in N-fixing
17 bacteria (Bothe et al., 2010), a small efflux of H_2 could help to fuel other autotrophic
18 metabolisms including both NO_3^- reduction (Nakagawa et al., 2005) or the Knallgas reaction (H_2
19 + O_2), perhaps providing some mutualistic benefit. Hydrogen-based metabolism has been
20 proposed as a significant contributor to subsurface autotrophy underlying the oligotrophic South
21 Pacific Gyre (D'Hondt et al., 2009). Although the involvement of so-called alternative
22 nitrogenases (the Fe and V forms), which have been shown to display an even larger kinetic
23 isotope effect (-6 to -7‰) than the Mo-bearing form (Zhang et al., 2014), could offer even
24 greater leverage on lowering of the bulk $\delta^{15}\text{N}$ (and source of N for nitrification), their
25 involvement in non-sulfidic marine systems, where Mo is replete and soluble Fe and V is scarce,
26 is expected to be minimal (Zhang et al., 2014). A similar argument was also made for the cryptic
27 involvement of N_2 fixation as source of low $\delta^{15}\text{N}$ and explanation for dual NO_3^- isotopic patterns
28 in the large oxygen minimum zone of eastern tropical North Pacific (Sigman et al., 2005). Thus,
29 we conclude that the low predicted values of $\delta^{15}\text{N}_{\text{NTR}}$ provide compelling evidence for an
30 important role of *in situ* N_2 fixation in these organic lean sediments.

1 Finally, there is a conspicuous increase in the predicted $\delta^{15}\text{N}_{\text{NTR}}$ at sites 2B and 3D (up
2 to +1.8 and +1.1‰, respectively) between 15-35m. Although we have no compelling explanation
3 for these observations, it is interesting that these values coincide with the transitional intervals
4 over which $\delta^{18}\text{O}_{\text{NO}_3}$ values increase much more rapidly than $\delta^{15}\text{N}_{\text{NO}_3}$. While it is possible that
5 our model is insufficient for constraining the isotope dynamics at NP, it may also be that these
6 suboxic depths support differential amounts of *in situ* nitrogen fixation leading to shifts in the
7 bulk $\delta^{15}\text{N}$ available for oxidation by nitrification.

8 The contribution of competitive branching during NH_4^+ consumption notwithstanding,
9 the predicted $\delta^{15}\text{N}_{\text{NTR}}$ values can serve as an index of the degree of organic matter deriving from
10 *in situ* N_2 fixation versus delivery from the overlying water ($\delta^{15}\text{N} \sim +3.7\text{‰}$). Indeed, using a
11 value of -2‰ to represent organic matter derived from biological N_2 fixation (Delwiche et al.,
12 1979; Meador et al., 2007; Minigawa and Wada, 1986), our results suggest that between 25 and
13 100% (with an average of $80 \pm 20\%$) of the organic nitrogen supply in these sediments derives
14 from biological nitrogen fixation, representing a potentially enormous relative role for *in situ*
15 autotrophy in sustaining these microbial communities. Under an assumption of steady state, and
16 ignoring a potential contribution of competitive branching in NH_4^+ consumption, rates of N_2
17 fixation were estimated as a fraction of nitrification and ranged up to $345 \text{ nmol cm}^{-3} \text{ yr}^{-1}$ (Table
18 1). The distribution of N_2 fixation rates were generally similar to nitrification – with much lower
19 rates ($8 - 45 \text{ nmol cm}^{-3} \text{ yr}^{-1}$) at site 4A – again consistent with overall lower cell abundance
20 (Zhao and Jørgensen, in review). These rates are 2-3 orders of magnitude lower than rates
21 measured in coastal and estuarine sediments (e.g., Bertics et al., 2010; Rao and Charette,
22 2012; Joye and Paerl, 1993), although still much higher than rates measured in studies of N_2
23 fixation in oligotrophic water column (e.g., Montoya et al., 2004; Capone et al., 2005). Overall,
24 North Pond sediments appear to harbor a spectrum of microbially mediated N transformations,
25 with rates lower than those found in most sedimentary systems, yet still generally higher than
26 those observed in overlying oligotrophic waters. Thus, while the influence of both sediment
27 hosted N_2 fixation and competitive branching during NH_4^+ consumption may not be mutually
28 exclusive, our analysis places important upper limits on the nature of autotrophic lifestyles
29 (including N_2 fixation) and the nitrogen economy in the deep subsurface.

30 **4.2.3 Model predicted values of the $\delta^{18}\text{O}$ of nitrification ($\delta^{18}\text{O}_{\text{NTR}}$)**

1 We also observed variation in estimated values of the $\delta^{18}\text{O}$ of newly produced NO_3^-
2 ($\delta^{18}\text{O}_{\text{NTR}}$), ranging from -2.8 to as high as +4.1‰ (at the O_2 minimum in 3D), which may offer
3 some insight into the nature of nitrification in these sediments and the deep ocean in general. The
4 oxygen isotope composition of newly produced NO_3^- reflects the combination of several
5 complex factors including 1) the $\delta^{18}\text{O}$ of the ambient water and dissolved O_2 , 2) kinetic isotope
6 effects during the enzymatically catalyzed incorporation of O atoms during oxidation of NH_4^+
7 and NO_2^- , as well as 3) the potential influence of oxygen isotope equilibration between water and
8 NO_2^- (both abiotic and/or that catalyzed by activity of microbial nitrifying bacteria) (Casciotti et
9 al., 2010).

10 In the upper profile of site 2B and throughout the profile of site 4A predicted values of
11 $\delta^{18}\text{O}_{\text{NTR}}$ clustered between -2.8 and 0.0‰ with no clear trends related to down core
12 concentrations of O_2 or NO_3^- (Figure 6). Although slightly lower, this range of values agrees
13 remarkably well with values predicted by experiments using a co-culture of NH_4^+ and NO_2^-
14 oxidizing bacteria, which ranged from -1.5 to +1.3‰ (Buchwald et al., 2012). In systems where
15 NH_4^+ and NO_2^- oxidizing bacteria co-exist and are not substrate-limited, NO_2^- does not generally
16 accumulate and the importance of oxygen isotope equilibration between NO_2^- and water can be
17 considered minor ($\sim 3\%$) (Buchwald et al., 2012). In this case, the $\delta^{18}\text{O}_{\text{NTR}}$ is primarily set by the
18 $\delta^{18}\text{O}$ of water (seawater $\delta^{18}\text{O} \sim 0\%$) and dissolved O_2 ($\sim +26.4\%$ for the deep N. Atlantic;
19 (Kroopnick et al., 1972)) and the three kinetic isotope effects during the sequential oxidation of
20 NH_4^+ to NO_3^- (Buchwald et al., 2012; Casciotti et al., 2010). The resulting $\delta^{18}\text{O}_{\text{NTR}}$ can be
21 described as:

$$22 \quad \delta^{18}\text{O}_{\text{NTR}} = 1/3[\delta^{18}\text{O}_{\text{O}_2} - ({}^{18}\epsilon_{\text{O}_2})] + 1/3[\delta^{18}\text{O}_{\text{water}} - ({}^{18}\epsilon_{\text{H}_2\text{O},1})] + 1/3[\delta^{18}\text{O}_{\text{water}} - {}^{18}\epsilon_{\text{H}_2\text{O},2}] \quad [11]$$

23 where ${}^{18}\epsilon$ is the kinetic isotope effect of O atom incorporation from O_2 during NH_4^+ oxidation to
24 NH_2OH (${}^{18}\epsilon_{\text{O}_2}$), and from water during NH_2OH oxidation to NO_2^- (${}^{18}\epsilon_{\text{H}_2\text{O},1}$) and NO_2^- oxidation to
25 NO_3^- (${}^{18}\epsilon_{\text{H}_2\text{O},2}$) (Buchwald et al., 2012).

26 While the value of seawater $\delta^{18}\text{O}$ can be considered to be relatively constant ($\sim 0\%$) in
27 North Pond porewaters, the respiratory consumption of O_2 , as evident in the observed
28 concentration profiles, imparts a relatively strong isotopic fractionation (Bender,

1 1990; Kroopnick and Craig, 1976; Lehmann et al., 2009) and will cause elevated $\delta^{18}\text{O}_{\text{O}_2}$ values.
2 Using a separate reaction-diffusion model (not shown) we estimated the $\delta^{18}\text{O}_{\text{O}_2}$ to be as high as
3 +70‰ where concentrations of O_2 have been drawn down >95% of the level found in bottom
4 seawater. Incorporation of this highly ^{18}O -enriched O_2 by nitrification in these low O_2 intervals
5 may contribute to observed increases in $\delta^{18}\text{O}_{\text{NTR}}$ predicted by our model. In particular, in the low
6 O_2 intervals of 2B and 3D, $\delta^{18}\text{O}_{\text{NTR}}$ values as high as +4.1‰ at the four intervals coinciding with
7 the maximum O_2 drawdown (Figure 6), and thus may point to incorporation of high- $\delta^{18}\text{O}$ O_2 . For
8 example, assuming a $\delta^{18}\text{O}$ value of 0‰ for seawater, using Eq. 11 and a combined isotope effect
9 of 18‰ for the two steps of NH_4^+ oxidation to NO_2^- ($^{18}\epsilon_{\text{O}_2} + ^{18}\epsilon_{\text{H}_2\text{O},1}$; the two have not yet been
10 resolved from one another; (Casciotti et al., 2010)) and a value of 15‰ for $^{18}\epsilon_{\text{H}_2\text{O},2}$ (O atom
11 incorporation during NO_2^- oxidation to NO_3^- , (Buchwald et al., 2012)), $\delta^{18}\text{O}_{\text{NTR}}$ values of -2‰,
12 +2‰ or +6‰ would imply incorporation of O from an O_2 pool with a value of \sim +45‰, +57‰ or
13 +69‰, respectively.

14 If these higher values are indeed the result of enriched O_2 incorporation, then they also
15 provide indirect information on the degree of oxygen isotope equilibration occurring between
16 NO_2^- and water. Specifically, if some proportion of an elevated $\delta^{18}\text{O}_{\text{O}_2}$ signal is propagated into
17 the NO_3^- pool, then this suggests that the intermediate NO_2^- pool did not completely equilibrate
18 with ambient water (which would effectively erase all signs of precursor molecule $\delta^{18}\text{O}$). Within
19 these low O_2 transitional intervals in 2B and 3D, it appears that the turnover of the very small
20 NO_2^- intermediate pool may be faster than the time required for complete equilibration between
21 NO_2^- and water (Buchwald and Casciotti, 2013). In contrast, the low O_2 interval from site 4A
22 does not exhibit elevated $\delta^{18}\text{O}_{\text{NTR}}$ values near the oxygen minimum, perhaps suggesting that the
23 turnover of NO_2^- here is slower (allowing complete equilibration) or that equilibration is
24 biologically catalyzed (e.g., enhanced by enzymatic activity (Buchwald et al., 2012)). Although
25 the concentrations of the NO_2^- pool were generally below detection, making the accurate
26 determination of its turnover time impossible (via $\delta^{18}\text{O}$), the use of NO_2^- oxygen isotopes as an
27 independent measure of metabolic processes where concentrations persist at measurable levels
28 may be a potentially powerful indicator of biological turnover of NO_2^- ($\delta^{15}\text{N}$ and $\delta^{18}\text{O}$ of NO_2^- in
29 2B, where NO_2^- was detected at two depths, were not determined as part of this study). Future

1 studies should target this pool as a complementary dimension for constraining subsurface
2 biosphere metabolic rates.

3 ***4.2.4 Model sensitivity to prescribed $^{15}\epsilon_{\text{DNF}}$ in transitional intervals***

4 In the transitional intervals, where both nitrification and denitrification are allowed to co-
5 occur, the model is underdetermined and requires some variables to be prescribed. We chose to
6 prescribe a value for the kinetic isotope effect of denitrification ($^{15}\epsilon_{\text{DNF}}$) and here examine the
7 sensitivity of estimated rates nitrification and denitrification, as well as predicted values of
8 $\delta^{15}\text{N}_{\text{NTR}}$ and $\delta^{18}\text{O}_{\text{NTR}}$. Given the rather tightly confined range of determined values for $^{15}\epsilon_{\text{DNF}}$ in
9 the anoxic zone of site 2B, averaging $20 \pm 1.8\%$, for illustration, we bracket our prescribed
10 $^{15}\epsilon_{\text{DNF}}$ in transitional intervals with values of 15 and 25‰ (rate estimates where the prescribed
11 $^{15}\epsilon_{\text{DNF}}$ is as low as 5‰ are given in Table 1). Overall, the model-predicted rates of nitrification
12 and denitrification, as well as values of $\delta^{15}\text{N}_{\text{NTR}}$ and $\delta^{18}\text{O}_{\text{NTR}}$ were largely insensitive to changes
13 in the prescribed strength of the isotope effect for denitrification ($^{15}\epsilon_{\text{DNF}}$) (Figure 4).

14 Specifically, when the prescribed value of $^{15}\epsilon_{\text{DNF}}$ decreased from 25‰ to 15‰, changes
15 in the predicted values of $\delta^{15}\text{N}_{\text{NTR}}$ and $\delta^{18}\text{O}_{\text{NTR}}$ were generally small (Figures 5 and 6), varying
16 by a maximum of 0.9‰ (average 0.5‰) and 2.3‰ (difference 0.6‰), respectively. An exception
17 to this are the intervals bracketing the anoxic zone of the profile at site 2B (at depths of 27.9m
18 and 70.8, 72.9m), which yielded predicted $\delta^{15}\text{N}_{\text{NTR}}$ that were either 2.1‰ lower (at 27.9m) or
19 ~5‰ higher (at 70.8m and 72.9m). Predicted $\delta^{18}\text{O}_{\text{NTR}}$ values were also quite sensitive to $^{15}\epsilon_{\text{DNF}}$ in
20 this interval with values that were 3.8‰ (at 27.9m) and 7.2-8.0‰ higher (at 70.8m and 72.9m).
21 While we cannot rule out the potential influence of changes in physiological expression of
22 isotope effects, the sensitivity of $\delta^{15}\text{N}_{\text{NTR}}$ and $\delta^{18}\text{O}_{\text{NTR}}$ to $^{15}\epsilon_{\text{DNF}}$ at these depths may point to an
23 unresolvable artifact of this model approach. Further work being indicated, incorporation of dual
24 nitrite isotopes could certainly aid in resolving this apparent sensitivity. However, this sensitivity
25 was not observed in the other transitional intervals of 2B, 3D or 4A and conclusions regarding
26 $\delta^{15}\text{N}_{\text{NTR}}$ and $\delta^{18}\text{O}_{\text{NTR}}$ still appear robust.

27 Finally, although literature values of $^{15}\epsilon_{\text{DNF}}$ almost uniformly fall between values of 13
28 and 30‰, values of $^{15}\epsilon_{\text{DNF}}$ as low as 2-5‰ have been observed occasionally in culture studies

1 (Granger et al., 2008; Wada et al., 1975). While we have no direct evidence that such low values
2 would be relevant in our study, we report the sensitivity of rate estimates and $\delta^{15}\text{N}_{\text{NTR}}$ and
3 $\delta^{18}\text{O}_{\text{NTR}}$ (Table 1). In short, a prescribed value for $^{15}\epsilon_{\text{DNF}}$ of 5‰ leads to increased estimates of
4 $\delta^{15}\text{N}_{\text{NTR}}$ and $\delta^{18}\text{O}_{\text{NTR}}$ by an average of 2.3‰ and 1.4‰, respectively (Figures 5 and 6). These
5 higher estimates of $\delta^{15}\text{N}_{\text{NTR}}$ would implicitly require a lower contribution of N_2 fixation derived
6 nitrogen as argued for above, though not eliminate its role completely, especially in 4A where
7 $\delta^{15}\text{N}_{\text{NTR}}$ values remain between -1 to +1‰ (Figure 5). While rates of nitrification were less
8 sensitive (somewhat higher in the upper layers of 4A), this very low prescribed value of $^{15}\epsilon_{\text{DNF}}$
9 often lead to dramatically increased estimates of denitrification rates – in particular in the upper
10 transitional layers of profiles at 2B and 3D where ~10-20 fold higher maximum denitrification
11 rates are required to reconcile nitrate concentration and isotope data (Table 1).

12 **4.2.5 Model-predicted values of $^{18}\epsilon:^{15}\epsilon_{\text{DNF}}$ and $^{15}\epsilon_{\text{DNF}}$**

13 In the anoxic intervals, estimated values of $^{18}\epsilon:^{15}\epsilon_{\text{DNF}}$ ranged from 0.83 to 1.11 with an
14 average value of 0.99 ± 0.1 (Table 2), consistent with a prominent role of respiratory nitrate
15 reductase (Nar), which imparts a $^{18}\epsilon:^{15}\epsilon_{\text{DNF}}$ of $\sim 0.96 \pm 0.01$ (Granger et al., 2008). Notably,
16 however, the lower values of 0.86 and 0.83 observed near the top and the core of the anoxic zone
17 in site 2B could suggest influence of nitrate reduction by periplasmic nitrate reductase (NAP)
18 (Granger et al., 2008) and chemolithotrophic NO_3^- reduction (Frey et al., 2014; Wenk et al., 2014),
19 which has been shown to impart a lower $^{18}\epsilon:^{15}\epsilon_{\text{DNF}}$ closer to 0.6. In this particular interval, this
20 could suggest that as much as 43% of nitrate reduction is chemolithotrophic and perhaps
21 metabolically linked to the oxidation of inorganic substrates such as reduced iron or sulfur
22 species. Although outside the scope of this study, interrogation of genetic markers of respiratory
23 and periplasmic nitrate reductase could shed more light on the role nitrate use by subsurface
24 microbial communities.

25 As discussed above, the model-estimated values of $^{15}\epsilon_{\text{DNF}}$ (averaging $20.0\% \pm 1.8\%$;
26 Table 2) at site 2B are quite consistent with values from a wide range of studies (Granger et al.,
27 2008), and references therein). Notably however, a different pattern emerges from the two anoxic
28 intervals of site 4A. Although model-estimated values of $^{15}\epsilon_{\text{DNF}}$ were unresolvable at 38.8m
29 (likely because the changes in $\delta^{15}\text{N}$ and $\delta^{18}\text{O}$ were too small for reliable model fits), estimated

1 $^{15}\epsilon_{\text{DNF}}$ values at 44.1m were $\sim 8.1 \pm 0.4\%$, much lower than observed in 2B. In general, the
2 values observed in 2B are consistent with observations from other environments hosting
3 denitrification (Granger et al., 2008), and suggest that denitrifying organisms may be adapted to
4 low levels of carbon (here $<0.2\%$ sediment organic carbon) and that their physiological poise
5 may be similar to those found in other anaerobic environments (albeit adapted to grow at
6 exceedingly slow nitrate reduction rates). However, the lower estimated $^{15}\epsilon_{\text{DNF}}$ values in 4A
7 might also reflect something else. Given the apparent low reactivity of the sediments of site 4A,
8 it is also possible that these particularly low $^{15}\epsilon_{\text{DNF}}$ values stem from denitrification operating
9 under extreme physiological energy limitation – as discussed below.

10 While a number of studies have shown that the apparent N isotopic effect for nitrate
11 reduction by denitrification can vary from 5 to 30‰ (e.g., (Barford et al., 1999; Delwiche and
12 Steyn, 1970; Granger et al., 2008), recent evidence suggests these variations are largely regulated
13 by changes in the combination of cellular uptake and efflux of NO_3^- leading to the expression (or
14 repression) of the enzyme level isotope effect outside the cell (Granger et al., 2008; Kritee et al.,
15 2012; Needoba et al., 2004). For example, at low extracellular NO_3^- concentrations – low $^{15}\epsilon_{\text{DNF}}$
16 values suggest that nitrate transport (having a low $^{15}\epsilon$) becomes the rate-limiting step (Granger et
17 al., 2008; Lehmann et al., 2007; Shearer et al., 1991). In North Pond porewaters, however, at
18 depths where O_2 is low enough for denitrification to occur, NO_3^- concentrations remain well
19 above $30\mu\text{M}$, a threshold well above the K_m for NO_3^- transporters ($2\text{-}18\mu\text{M}$; (Parsonage et al.,
20 1985; Murray et al., 1989; Zumft, 1997)), suggesting that low $^{15}\epsilon_{\text{DNF}}$ due to transport limitation of
21 NO_3^- reduction is unlikely.

22 In general, greater expression of the intrinsic enzymatic isotope effect (e.g., higher
23 observed $^{15}\epsilon_{\text{DNF}}$) should occur under conditions in which there is a higher efflux of intracellular
24 NO_3^- relative to NO_3^- uptake (Kritee et al., 2012). Interestingly, this efflux/uptake ratio appears
25 to be linked to nitrate reduction rates in denitrifying bacteria, with lower cell-specific nitrate
26 reduction rates leading to lower efflux/uptake ratios and lower observed cellular level $^{15}\epsilon_{\text{DNF}}$
27 (Kritee et al., 2012). Indeed, evidence seems to indicate that this efflux/uptake ratio in
28 denitrifying bacteria is highly regulated and that NO_3^- uptake is sensitive to cellular level energy
29 supply. For example, under conditions in which organisms are required to maintain a careful

1 regulation of energetically costly metabolic processes, it is logical that there would be a lower
2 density of NO_3^- transporters and that intracellular NO_3^- concentrations would be maintained at or
3 near optimal levels for reduction by nitrate reductase. Similarly, growth under energy-poor
4 carbon substrate supply may also lead to lower observed $^{15}\epsilon_{\text{DNF}}$, due to an energy-driven decrease
5 in NO_3^- uptake, lower intracellular NO_3^- concentrations and a lower efflux/uptake ratio.

6 We suggest that the difference between the lower $^{15}\epsilon_{\text{DNF}}$ value estimated from the anoxic
7 interval of 4A and the more ‘conventional’ values from deeper within anoxic intervals of 2B
8 could stem from physiological-level controls on the cellular level expression of $^{15}\epsilon_{\text{DNF}}$.
9 Specifically, as all porewater evidence from site 4A (O_2 , NO_3^- , N and O isotopes) indicates
10 substantially lower levels of microbial activity, denitrification may actually be more energy-
11 limited by carbon (compared to denitrification in the deeper intervals of 2B). This suggests that
12 the operation of denitrification under extremely carbon-poor environments (4A) may lead to
13 conditions where the enzyme-level N isotope fractionation of denitrification is under-expressed
14 on both the cellular, and ecosystem levels, and $^{15}\epsilon_{\text{DNF}}$ values are much lower than commonly
15 encountered under even just slightly more energy-replete conditions (e.g., 2B).

16 **5. SUMMARY**

17 In summary, the porewater nitrate isotopic composition reflects the active redox cycling
18 of nitrogen by the subsurface microbial community – including both oxidative and reductive
19 transformations. The variations in reaction rates across and within the three North Pond sites are
20 generally consistent with the distribution of dissolved oxygen, but not necessarily with the
21 canonical view of how redox thresholds act to spatially separate nitrate regeneration from
22 dissimilatory consumption (e.g., denitrification). The incorporation of nitrate dual isotopes into
23 an inverse reaction-diffusion model provides evidence for extensive zones of overlap where O_2
24 and NO_3^- respiration (nitrification and denitrification) co-occur. The isotope modeling also
25 yielded estimates for the $\delta^{15}\text{N}$ and $\delta^{18}\text{O}$ of newly produced nitrate ($\delta^{15}\text{N}_{\text{NTR}}$ and $\delta^{18}\text{O}_{\text{NTR}}$), as well
26 as the isotope effect for denitrification ($^{15}\epsilon_{\text{DNF}}$), parameters with high relevance to global ocean
27 models of N cycling (Sigman et al., 2009). Estimated values of $\delta^{15}\text{N}_{\text{NTR}}$ were generally lower
28 than previously reported $\delta^{15}\text{N}$ values for sinking PON in this region, suggesting the potential
29 influence of sedimentary N_2 fixation and remineralization/oxidation of the newly fixed organic N.

1 Model estimated values of $\delta^{18}\text{O}_{\text{NTR}}$ generally ranged between -2.8 and 0.0‰, consistent with lab
2 studies of nitrifying bacteria cultures. Notably, however, some $\delta^{18}\text{O}_{\text{NTR}}$ values were elevated,
3 suggesting incorporation of ^{18}O -enriched dissolved oxygen during the nitrification process, and
4 implying relatively rapid rates of nitrite turnover in environments supporting nitrification. In
5 contrast, the accumulation of NO_2^- under denitrifying conditions likely reflects limitation of NO_2^-
6 reduction by organic matter availability and generally low rates of N-based heterotrophic
7 respiration. Importantly, our findings indicate that the production of organic matter by *in situ*
8 autotrophy (e.g., nitrification and nitrogen fixation) must supply a substantial fraction of the
9 biomass and organic substrate for heterotrophy in these sediments, supplementing the small
10 organic matter pool derived from the overlying euphotic zone. Thus, despite exceedingly low
11 exogenous organic matter input, this work sheds new light on an active nitrogen cycle in the
12 deep sedimentary biosphere underlying half of the global ocean.

1 **FIGURE CAPTIONS**

2 **Figure 1.** Map of North Pond study site (created using the default Multi-Resolution Topography
3 Synthesis base map in GeoMapApp ver. 3.5.1). Color scale reflects water depth in meters with
4 contour intervals of 100m.

5 **Figure 2.** Depth profiles from IODP sites U1382B, U1383D and U1384A at North Pond of
6 porewater concentrations of O₂ (from Orcutt *et al.*, 2013) and NO₃⁻ as well as the N and O
7 isotopic composition of NO₃⁻. ($\delta^{15}\text{N}_{\text{NO}_3}$ and $\delta^{18}\text{O}_{\text{NO}_3}$). The red circle at the top of the profiles
8 denotes the bottom seawater NO₃⁻ concentration of 21.6 μM (Ziebis *et al.*, 2012). Horizontal
9 black lines indicate depth of contact with ocean crust. Gray boxes indicate ‘transitional’ zones in
10 which a reaction-diffusion model is used to calculate co-occurring nitrification and
11 denitrification (see text for details). Strong increases in $\delta^{15}\text{N}$ and $\delta^{18}\text{O}$ in U1382B coincide with
12 depths having the lowest O₂ concentration and are indicative of the influence of denitrification.
13 While the NO₃⁻ concentrations profiles of U1383D and U1384A appear similar, stark differences
14 in the nitrate dual isotopic composition reflect the generally low level of microbial activity in
15 U1384A.

16 **Figure 3.** Dual isotope plot illustrating the relationship between $\delta^{15}\text{N}_{\text{NO}_3}$ and $\delta^{18}\text{O}_{\text{NO}_3}$ in North
17 Pond porewaters. The diagonal line, rooted at a value for bottom seawater ($\delta^{15}\text{N}$ of +5.5‰ and
18 $\delta^{18}\text{O}$ of +1.8‰), depicts a 1:1 slope representative of the expected change in $\delta^{15}\text{N}$ and $\delta^{18}\text{O}$ by
19 the process of denitrification alone. Trends falling well above this 1:1 line, together with the
20 concentration profiles reflect the combined role of nitrification in these porewaters.

21 **Figure 4.** Model estimated rates of denitrification and nitrification ($\text{nmol cm}^{-3} \text{ yr}^{-1}$) based on
22 fitting of nitrate concentration and N and O isotopic composition. Estimates within transitional
23 intervals are calculated using a value for $^{15}\epsilon_{\text{DNF}}$ of either 15‰ (dashed) or 25‰ (solid). Error
24 bars are shown for the $^{15}\epsilon_{\text{DNF}} = 25\text{‰}$ only and indicate the standard error of 10 model runs (see
25 text). Note the different scales for rates among the three profiles.

26 **Figure 5.** Model estimated values for the N isotopic composition of new nitrate produced by
27 nitrification ($\delta^{15}\text{N}_{\text{NTR}}$) occurring within porewaters. Values are calculated for depths at which O₂
28 concentrations were $>2\mu\text{M}$ (e.g., oxic and transitional intervals). Sensitivity of $\delta^{15}\text{N}_{\text{NTR}}$ to

1 prescribed values of the isotope effect for denitrification ($^{15}\epsilon_{\text{DNF}}$) in transitional intervals, where
2 both nitrification and denitrification can co-occur, is also indicated.

3 **Figure 6.** Model estimated values for the O isotopic composition of new nitrate produced by
4 nitrification ($\delta^{18}\text{O}_{\text{NTR}}$) occurring within porewaters. Values are calculated for depths at which O_2
5 concentrations were $>2\mu\text{M}$ (e.g., oxic and transitional intervals). Sensitivity of $\delta^{18}\text{O}_{\text{NTR}}$ to
6 prescribed values of the isotope effect for denitrification ($^{15}\epsilon_{\text{DNF}}$) in transitional intervals, where
7 both nitrification and denitrification can co-occur, is also indicated.

8

1 **AUTHOR CONTRIBUTIONS**

2 SW, WZ, CW, and ML conceived of the study. SW and WZ procured funding to carry
3 out the presented work. CW and WZ participated in the IODP Expedition 336 as shore-based
4 scientists, received and analyzed samples. SW collected samples from frozen archives. SW
5 analyzed the samples, developed the model, and interpreted the model results with assistance
6 from CB and ML. SW wrote the paper with input from CB, WZ, CW and ML. All authors
7 discussed the paper and commented on the final manuscript.

1 **ACKNOWLEDGEMENTS**

2 The authors would like to acknowledge the entire shipboard party of the IODP
3 Expedition 336 for their unflagging efforts during the drilling and collection of these North Pond
4 sediment profiles. We would also like to thank Mark Rollog and Zoe Sandwith for assistance
5 with the isotope and concentration measurements at University of Basel and at WHOI,
6 respectively. SW thanks David Glover for stimulating conversations about model formulations.
7 Funding for this work was provided in part by the International Ocean Drilling Program, Woods
8 Hole Oceanographic Institution and a grant from the Center for Dark Energy Biosphere
9 Investigations (C-DEBI) to SW and WZ and a postdoc fellowship to CB from C-DEBI. WZ was
10 supported in part by NSF grant OCE-1131671. This is C-DEBI contribution number #####.

1 REFERENCES

- 2 Altabet, M. A.: Variations in nitrogen isotopic composition between sinking and suspended
3 particles: Implications for nitrogen cycling and particle transformations in the open ocean,
4 Deep Sea Research Part I, 35, 535-554, 1988.
- 5 Altabet, M. A.: A time-series study of the vertical structure of nitrogen and particle
6 dynamics in the Sargasso Sea, Limnology and Oceanography, 34, 1185-1201, 1989.
- 7 Altabet, M. A., Pilskaln, C., Thunell, R. C., Pride, C., Sigman, D. M., Chavez, F. P., and Francois,
8 R.: The nitrogen isotope biogeochemistry of sinking particles from the margin of the
9 Eastern North Pacific, Deep Sea Research I, 46, 655-679, 1999.
- 10 Andersson, K. K., and Hooper, A. B.: O₂ and H₂O are each the source of one O in NO₂
11 produced from NH₃ by Nitrosomonas: ¹⁵N-NMR evidence, FEBS Letters, 164, 236-240,
12 1983.
- 13 Barford, C. C., Montoya, J. P., Altabet, M. A., and Mitchell, R.: Steady-state Nitrogen Isotope
14 Effects of N₂ and N₂O Production in *Paracoccus denitrificans*, Applied and Environmental
15 Microbiology, 65, 989-994, 1999.
- 16 Becker, K., Langseth, M., and Hyndman, R.: Temperature measurements in Hole 395A, Leg
17 78B, Washington DC, 689-698, 1984.
- 18 Becker, K., Bartetzko, A., and Davis, E. E.: Leg 174B Synopsis: Revisiting Hole 395A for
19 Logging and Long-term Monitoring of Off-axis Hydrothermal Processes in Young Ocean
20 Crust, 1-13, 2001.
- 21 Bender, M. L.: The $\delta^{18}\text{O}$ of dissolved O₂ in seawater: A unique tracer of circulation and
22 respiration in the deep sea, Journal of Geophysical Research, 95, 22243-22252, 1990.
- 23 Berelson, W. M., Hammond, D. E., O'Neill, D., Xu, X.-M., Chin, C., and Zuckin, J.: Benthic fluxes
24 and pore water studies from sediments of the central equatorial north Pacific: Nutrient
25 diagenesis, Geochimica et Cosmochimica Acta, 54, 3001-3012, 1990.
- 26 Bertics, V. J., Sohm, J. A., Treude, T., Chow, C.-E., Capone, D. G., Fuhrman, J. A., and Ziebis, W.:
27 Burrowing deeper into benthic nitrogen cycling: The impact of bioturbation on nitrogen
28 fixation coupled to sulfate reduction, Marine Ecology Progress Series, 409, 1-15, 2010.
- 29 Blair, N. E., and Aller, R. C.: The fate of terrestrial organic carbon in the marine environment,
30 Annual Review of Marine Science, 4, 401-423, doi:10.1146/annurev-marine-120709-
31 142717, 2012.
- 32 Bothe, H., Schmitz, O., Yates, M. G., and Newton, W. E.: Nitrogen fixation and hydrogen
33 metabolism in cyanobacteria, Microbiology and Molecular Biology Reviews, 74, 529-551,
34 2010.
- 35 Braman, R. S., and Hendrix, S. A.: Nanogram nitrite and nitrate determination in
36 environmental and biological materials by vanadium (III) reduction with
37 chemiluminescence detection, Analytical Chemistry, 61, 2715-2718, 1989.
- 38 Brewer, P. G., Hofmann, A. F., Peltzer, E. T., and Ussler III, W.: Evaluating microbial chemical
39 choices: The ocean chemistry basis for the competition between use of O₂ or NO₃⁻ as an
40 electron acceptor, Deep-Sea Research I, 87, 35-42, 2014.
- 41 Buchwald, C., and Casciotti, K. L.: Oxygen isotopic fractionation and exchange during
42 bacterial nitrite oxidation, Limnology and Oceanography, 55, 1064-1074, 2010.

1 Buchwald, C., Santoro, A. E., McIlvin, M. R., and Casciotti, K. L.: Oxygen isotopic composition
2 of nitrate and nitrite produced by nitrifying cocultures and natural marine assemblages,
3 *Limnology and Oceanography*, 57, doi:10.4319/lo.2012.57.5.0000, 2012.

4 Buchwald, C., and Casciotti, K. L.: Isotopic ratios of nitrite as tracers of the sources and age
5 of oceanic nitrite, *Nature Geoscience*, 6, 309-313, 2013.

6 Capone, D. G., Burns, J. A., Montoya, J. P., Subramaniam, A., Mahaffey, C., Gunderson, T.,
7 Michaels, A. F., and Carpenter, E. J.: Nitrogen fixation by *Trichodesmium* spp.: An important
8 source of new nitrogen to the tropical and subtropical North Atlantic Ocean, *Global
9 Biogeochemical Cycles*, 19, GB2024, doi:10.1029/2004GB002331, 2005.

10 Casciotti, K. L., Sigman, D. M., Galanter-Hastings, M., Böhlke, J. K., and Hilkert, A.:
11 Measurement of the oxygen isotopic composition of nitrate in seawater and freshwater
12 using the denitrifier method, *Analytical Chemistry* 74, 4905-4912, 2002.

13 Casciotti, K. L., and McIlvin, M. R.: Isotopic analyses of nitrate and nitrite from reference
14 mixtures and application to Eastern Tropical North Pacific waters, *Marine Chemistry*, 107,
15 184-201, 2007.

16 Casciotti, K. L., Trull, T. W., Glover, D., and Davies, D.: Constraints on nitrogen cycling at the
17 subtropical North Pacific Station ALOHA from isotopic measurements of nitrate and
18 particulate nitrogen, *Deep Sea Research II*, 55, 1661-1672, 2008.

19 Casciotti, K. L., McIlvin, M., and Buchwald, C.: Oxygen isotopic exchange and fractionation
20 during bacterial ammonia oxidation, *Limnology and Oceanography*, 55, 753-762, 2010.

21 Christensen, J. P., and Rowe, G. T.: Nitrification and oxygen consumption in northwest
22 Atlantic deep-sea sediments, *Journal of Marine Research*, 42, 1099-1116, 1984.

23 Christensen, J. P., Murray, J. W., Devol, A. H., and Codispoti, L. A.: Denitrification in
24 continental shelf sediments has major impact on the ocean nitrogen budget, *Global
25 Biogeochemical Cycles*, 1, 97-116, 1987.

26 Clark, I., and Fritz, P.: *Environmental Isotopes in Hydrogeology*, CRC Press, Boca Raton,
27 Florida, 331 pp., 1997.

28 Cox, R. D.: Determination of nitrate and nitrite at the parts per billion level by
29 chemiluminescence, *Analytical Chemistry*, 52, 332-335, 1980.

30 D'Hondt, S., Spivack, A. J., Pockalny, R., Ferdelman, T. G., Fischer, J. P., Kallmeyer, J., Abrams,
31 L. J., Smith, D. C., Graham, D., Hasiuk, F., Schrum, H., and Stancin, A. M.: Subseafloor
32 sedimentary life in the South Pacific Gyre, *Proceedings of the National Academy of Sciences
33 of the United States of America*, 106, 11651-11656, 2009.

34 D'Hondt, S., Inagaki, F., Zarikian, C. A., Abrams, L. J., Dubois, N., Engelhardt, T., Evans, H.,
35 Ferdelman, T., Gribsholt, B., Harris, R. N., Hoppie, B. W., Hyun, J.-H., Kallmeyer, J., Kim, J.,
36 Lynch, J. E., McKinley, C. C., Mitsunobu, S., Morono, Y., Murray, R. W., Pockalny, R., Sauvage, J.,
37 Shimono, T., Shiraishi, F., Smith, D. C., Smith-Duque, C. E., Spivack, A. J., Steinsbu, B. O.,
38 Suzuki, Y., Szpak, M., Toffin, L., Uramoto, G., Yamaguchi, Y. T., Zhang, G.-l., Zhang, X.-H., and
39 Ziebis, W.: Presence of oxygen and aerobic communities from sea floor to basement in
40 deep-sea sediments, *Nature Geoscience*, 8, 299-303, 2015.

41 Davis, E. E., Becker, K., Pettigrew, T., Carson, B., and MacDonald, R.: CORK: A Hydrological
42 Seal and Downhole Observatory for Deep-Ocean Boreholes, 43-53, 1992.

43 Defforey, D., and Paytan, A.: Data Report: Characteristics of sedimentary phosphorus at
44 North Pond, IODP Expedition 336, Tokyo, Japan, 2015.

45 Delwiche, C., Zinke, P., Johnson, C., and Virginia, R.: Nitrogen isotope distribution as a
46 presumptive indicator of nitrogen fixation, *Botanical Gazette*, 140, 65-69, 1979.

1 Delwiche, C. C., and Steyn, P. L.: Nitrogen isotope fractionation in soils and microbial
2 reactions, *Environmental Science & Technology*, 4, 929-935, 1970.

3 Devol, A. H.: Direct measurement of nitrogen gas fluxes from continental shelf sediments,
4 *Nature*, 349, 319-321, 1991.

5 Edwards, K. J., Wheat, C. G., and Sylvan, J. B.: Under the Sea: Microbial Life in Volcanic
6 Oceanic Crust, *Nature Reviews in Microbiology*, 9, 703-712, 2011.

7 Edwards, K. J., Bach, W., Klaus, A., and Scientists, E.: Mid-Atlantic Ridge microbiology:
8 Initiation of long-term coupled microbiological, geochemical, and hydrological
9 experimentation within the seafloor at North Pond, western flank of the Mid-Atlantic Ridge,
10 Integrated Ocean Drilling Program Management International, Inc., Tokyo, Japan, 2012a.

11 Edwards, K. J., Becker, K., and Colwell, F.: The deep, dark energy biosphere: Intraterrestrial
12 life on Earth, *Annual Review of Earth and Planetary Science*, 40, 551-568,
13 doi:10.1146/annurev-earth-042711-105500, 2012b.

14 Estep, M. L. F., and Macko, S. A.: Nitrogen isotope biogeochemistry of thermal springs, *Org.*
15 *Geochem.*, 6, 779-785, 1984.

16 Expedition-336-Scientists: Mid-Atlantic Ridge microbiology: initiation of long-term coupled
17 microbiological, geochemical and hydrological experimentation within the seafloor at
18 North Pond, western flank of the Mid-Atlantic Ridge, 2012a.

19 Expedition-336-Scientists: Expedition 336 Summary, Tokyo, Japan, 2012b.

20 Fawcett, S. E., Ward, B. B., Lomas, M. W., and Sigman, D. M.: Vertical decoupling of nitrate
21 assimilation and nitrification in the Sargasso Sea, *Deep Sea Research Part I: Oceanographic*
22 *Research Papers*, 103, 64-72, 2015.

23 Fischer, J. P., Ferdelman, T. G., D'Hondt, S., Røy, H., and Wenzhöfer, F.: Oxygen penetration
24 deep into the sediment of the South Pacific gyre, *Biogeosciences*, 6, 1467-1478,
25 doi:10.5194/bg-6-1467-2009, 2009.

26 Frey, C., Heitanen, S., Jürgens, K., Labrenz, M., and Voss, M.: N and O isotope fractionation in
27 nitrate during chemolithoautotrophic denitrification by *Sulfurimonas gotlandica*,
28 *Environmental Science & Technology*, 48, 13229-13327, doi:10.1021/es503456g, 2014.

29 Gable, R., Morin, R., and Becker, K.: Geothermal state of DSDP Holes 333A, 395A and 534A:
30 Results from the DIANAUT program, *Geophysical Research Letters*, 19, 505-508, 1992.

31 Garside, C.: A chemiluminescent technique for the determination of nanomolar
32 concentrations of nitrate and nitrite in seawater, *Marine Chemistry*, 11, 159-167, 1982.

33 Goloway, F., and Bender, M. L.: Diagenetic models of interstitial nitrate profiles in deep sea
34 suboxic sediments, *Limnology and Oceanography*, 27, 624-638, 1982.

35 Granger, J., Sigman, D. M., Needoba, J. A., and Harrison, P. J.: Coupled nitrogen and oxygen
36 isotope fractionation of nitrate during assimilation by cultures of marine phytoplankton,
37 *Limnology and Oceanography*, 49, 1763-1773, 2004.

38 Granger, J., Sigman, D. M., Lehmann, M. F., and Tortell, P. D.: Nitrogen and oxygen isotope
39 fractionation during dissimilatory nitrate reduction by denitrifying bacteria, *Limnology and*
40 *Oceanography*, 53, 2533-2545, 2008.

41 Granger, J., and Sigman, D. M.: Removal of nitrite with sulfamic acid for nitrate N and O
42 isotope analysis with the denitrifier method, *Rapid Communications in Mass Spectrometry*,
43 23, 3753-3762, 2009.

44 Granger, J., Sigman, D. M., Rohde, M., Maldonado, M., and Tortell, P. D.: N and O isotope
45 effects during nitrate assimilation by unicellular prokaryotic and eukaryotic plankton
46 cultures, *Geochimica et Cosmochimica Acta*, 74, 1030-1040, 2010.

1 Granger, J., Prokopenko, M. G., Sigman, D. M., Mordy, C. W., Morse, Z. M., Morales, L.,
2 Sambrotto, R. N., and Plessen, B.: Coupled nitrification-denitrification in sediment of the
3 eastern Bering Sea shelf leads to ¹⁵N enrichment of fixed N in shelf waters, *Journal of*
4 *Geophysical Research*, 116, C11006, doi:10.1029/2010JC006751, 2011.

5 Grasshoff, K., Kremling, K., and Ehrhardt, M.: *Methods of Seawater Analysis*, 3 ed., Wiley,
6 2007.

7 Gruber, N.: The Marine Nitrogen Cycle Overview and Challenges, in: *Nitrogen in the Marine*
8 *Environment*, 2nd ed., edited by: Capone, D. G., Bronk, D. A., Mulholland, M. R., and
9 Carpenter, E. J., Elsevier, Amsterdam, Netherlands, 1-50, 2008.

10 Grundmanis, V., and Murray, J. W.: Aerobic respiration of pelagic marine sediments,
11 *Geochimica et Cosmochimica Acta*, 46, 1101-1120, 1982.

12 Hammond, D. E., McManus, J., Berelson, W. M., Kilgore, T. E., and Pope, R. H.: Early
13 diagenesis of organic material in equatorial Pacific sediments: stoichiometry and kinetics,
14 *Deep-sea Research II*, 43, 1365-1412, 1996.

15 Hoch, M. P., Fogel, M. F., and Kirchman, D. L.: Isotope fractionation associated with
16 ammonium uptake by a marine bacterium, *Limnology and Oceanography*, 37, 1447-1459,
17 1992.

18 Holmes, R., Aminot, A., Kerouel, R., Hooker, B., and Peterson, B. J.: A simple and precise
19 method for measuring ammonium in marine and freshwater ecosystems, *Canadian Journal*
20 *of Fish and Aquatic Science*, 56, 1801-1808, 1999.

21 Jahnke, R. A., Emerson, S. R., and Murray, J. W.: A model of oxygen reduction, denitrification,
22 and organic matter mineralization in marine sediments, *Limnology and Oceanography*, 27,
23 610-623, 1982.

24 Joye, S. B., and Paerl, H. W.: Contemporaneous nitrogen fixation and denitrification in
25 intertidal microbial mats - rapid response to runoff events, *Marine Ecology Progress Series*,
26 94, 267-274, 1993.

27 Karsh, K. L., Granger, J., Kritee, K., and Sigman, D. M.: Eukaryotic assimilatory nitrate
28 reductase fractionates N and O isotopes with a ratio near unity, *Environmental Science &*
29 *Technology*, 46, 5727-5735, doi:10.1021/es204593q, 2012.

30 Knapp, A. N., Sigman, D. M., and Lipschultz, F.: N isotopic composition of dissolved organic
31 nitrogen and nitrate at the Bermuda Atlantic Time-series Study site, *Global Biogeochemical*
32 *Cycles*, 19, doi:10.1029/2004GB002320, 2005.

33 Knapp, A. N.: The sensitivity of marine N₂ fixation to dissolved inorganic nitrogen, *Frontiers*
34 *in Microbiology*, doi:10.3389/fmicb.2012.00374, 2012.

35 Kritee, K., Sigman, D. M., Granger, J., Ward, B. B., Jayakumar, A., and Deutsch, C.: Reduced
36 isotope fractionation by denitrification under conditions relevant to the ocean, *Geochimica*
37 *et Cosmochimica Acta*, 92, 243-259, 2012.

38 Kroopnick, P., Weiss, R. F., and Craig, H.: Total CO₂, ¹³C, and dissolved oxygen ¹⁸O at
39 GEOSECS II in the North Atlantic, *Earth and Planetary Science Letters*, 16, 103-110, 1972.

40 Kroopnick, P., and Craig, H.: Oxygen isotope fractionation in dissolved oxygen in the deep
41 sea, *Earth and Planetary Science Letters*, 32, 375-388, 1976.

42 Langseth, M. G., Becker, K., von Herzen, R. P., and Schultheiss, P.: Heat and fluid flux through
43 sediment on the western flank of the Mid-Atlantic Ridge: A hydrogeological study of North
44 Pond, *Geophysical Research Letters*, 19, 517, 1992.

45 Lehmann, M. F., Bernasconi, S. M., Barbieri, A., and McKenzie, J. A.: Preservation of organic
46 matter and alteration of its carbon and nitrogen isotope composition during simulated and

1 in situ early sedimentary diagenesis, *Geochimica et Cosmochimica Acta*, 66, 3573-3584,
2 2002.

3 Lehmann, M. F., Sigman, D. M., and Berelson, W. M.: Coupling the $^{15}\text{N}/^{14}\text{N}$ and $^{18}\text{O}/^{16}\text{O}$ of
4 nitrate as a constraint on benthic nitrogen cycling, *Marine Chemistry*, 88, 1-20, 2004.

5 Lehmann, M. F., Sigman, D. M., McCorkle, D. C., Brunnelle, B. G., Hoffman, S., Kienast, M.,
6 Cane, G., and Clement, J.: Origin of the deep Bering Sea nitrate deficit: Constraints from the
7 nitrogen and oxygen isotopic composition of water column nitrate and benthic nitrate
8 fluxes, *Global Biogeochemical Cycles*, 19, GB4005, doi:10.1029/2005GB002508, 2005.

9 Lehmann, M. F., Sigman, D. M., McCorkle, D. C., Granger, J., Hoffman, S., Cane, G., and
10 Brunelle, B. G.: The distribution of nitrate $^{15}\text{N}/^{14}\text{N}$ in marine sediments and the impact of
11 benthic nitrogen loss on the isotopic composition of oceanic nitrate, *Geochimica et*
12 *Cosmochimica Acta*, 71, 5384-5404, 2007.

13 Lehmann, M. F., Barnett, B., Gelinas, Y., Gilbert, D., Maranger, R. J., Mucci, A., Sundby, B., and
14 Thibodeau, B.: Aerobic respiration and hypoxia in the Lower St. Lawrence Estuary: Stable
15 isotope ratios of dissolved oxygen constrain oxygen sink partitioning, *Limnology and*
16 *Oceanography*, 54, 2157-2169, 2009.

17 Li, Y.-H., and Gregory, S.: Diffusion of ions in sea water and in deep-sea sediments,
18 *Geochimica et Cosmochimica Acta*, 38, 703-714, 1974.

19 Marconi, D., Weigand, M. A., Rafter, P. A., McIlvin, M. R., Forbes, M., Casciotti, K. L., and
20 Sigman, D. M.: Nitrate isotope distributions on the US GEOTRACES North Atlantic cross-
21 basin section: Signals of polar nitrate sources and low latitude nitrogen cycling, *Marine*
22 *Chemistry*, in press, 2015.

23 Mason, O. U., Nakagawa, T., Rosner, M., van Nostrand, J. D., Zhou, J., Maruyama, A., Fisk, M. R.,
24 and Giovannoni, S. J.: First investigation of the microbiology of the deepest layer of ocean
25 crust, *PLoS One*, 5, doi:10.1371/journal.pone.0015399, 2010.

26 McIlvin, M., and Casciotti, K. L.: Technical updates to the bacterial method for nitrate
27 isotopic analyses, *Analytical Chemistry*, 83, 1850-1856, 2011.

28 McIlvin, M. R., and Casciotti, K. L.: Fully automated system for stable isotopic analyses of
29 dissolved nitrous oxide at natural abundance levels, *Limnology and Oceanography*:
30 *Methods*, 8, 54-66, 2010.

31 McManus, J., Hammond, D. E., Berelson, W. M., Kilgore, T. E., Demaster, D. J., Ragueneau, O.
32 G., and Collier, R. W.: Early diagenesis of biogenic opal: Dissolution rates, kinetics, and
33 paleoceanographic implications, *Deep Sea Research II*, 42, 871-903, 1995.

34 Meador, T. B., Aluwihare, L. I., and Mahaffey, C.: Isotopic heterogeneity and cycling of
35 organic nitrogen in the oligotrophic ocean, *Limnology and Oceanography*, 52, 934-947,
36 2007.

37 Minigawa, M., and Wada, E.: Nitrogen isotope ratios of red tide organisms in the East China
38 Sea: A characterization of biological nitrogen fixation, *Marine Chemistry*, 19, 245-259, 1986.

39 Montoya, J. P., Holl, C. M., Zehr, J. P., Hansen, A., Villareal, T. A., and Capone, D. G.: High rates
40 of N_2 fixation by unicellular diazotrophs in the oligotrophic Pacific ocean, *Nature*, 430,
41 1027-1032, doi:10.1038/nature02824, 2004.

42 Mosier, A. C., and Francis, C. A.: Relative abundance and diversity of ammonia-oxidizing
43 archaea and bacteria in the San Francisco Bay estuary, *Environmental Microbiology*,
44 doi:10.1111/j.1462-2920.2008.01764.x, 2008.

45 Murray, J. W., and Grundmanis, V.: Oxygen consumption in pelagic marine sediments,
46 *Science*, 209, 1527-1530, 1980.

1 Murray, R., Parsons, L., and Smith, M.: Kinetics of nitrate utilization by mixed populations of
2 denitrifying bacteria, *Applied and Environmental Microbiology*, 55, 717, 1989.

3 Nakagawa, S., Takai, K., Inagaki, F., Horikoshi, K., and Sako, Y.: *Nitratiruptor tergaricus* gen.
4 no., sp. nov. and *Nitratifractor salsuginis* gen. nov., sp. nov., nitrate-reducing
5 chemolithoautotrophs of the ϵ -Proteobacteria isolated from a deep-sea hydrothermal
6 system in the Mid-Okinawa Trough, *International Journal of Systematic and Evolutionary*
7 *Microbiology*, 55, 925-933, 2005.

8 Needoba, J. A., Sigman, D. M., and Harrison, P. J.: The mechanism of isotope fractionation
9 during algal nitrate assimilation as illuminated by the $^{15}\text{N}/^{14}\text{N}$ of intracellular nitrate,
10 *Journal of Phycology*, 40, 517-522, 2004.

11 Nunoura, T., Nishizawa, M., Kikuchi, T., Tsubouchi, T., Hirai, M., Koide, O., Miyazaki, J.,
12 Hirayama, H., Koba, K., and Takai, K.: Molecular biological and isotopic biogeochemical
13 prognoses of the nitrification-driven dynamic microbial nitrogen cycle in hadopelagic
14 sediments *Environmental Microbiology*, 15, 3087-3107, doi:10.1111/1462-2920.12152,
15 2013.

16 Orcutt, B. N., Sylvan, J. B., Knab, N. J., and Edwards, K. J.: Microbial Ecology of the Dark Ocean
17 above, at, and below the Seafloor, *Microbiology and Molecular Biology Reviews*, 75, 361-
18 422, 2011.

19 Orcutt, B. N., Wheat, C. G., Rouxel, O., Hulme, S., Edwards, K. J., and Bach, W.: Oxygen
20 consumption in subseafloor basaltic crust, *Nature*, 2013.

21 Parsonage, D., Greenfield, A. J., and Ferguson, S. J.: The high affinity of *Paracoccus*
22 *denitrificans* cells for nitrate as an electron acceptor. Analysis of possible mechanisms of
23 nitrate and nitrite movement across the plasma membrane and the basis for inhibition by
24 added nitrite of oxidase activity in permeabilised cells., *Biochimica et Biophysica Acta*, 807,
25 81-95, 1985.

26 Picard, A., and Ferdelman, T.: Linking microbial heterotrophic activity and sediment
27 lithology in oxic, oligotrophic sub-seafloor sediments of the North Atlantic Ocean, *Frontiers*
28 *in Microbiology*, 2, doi:10.3389/fmicb.2011.00263, 2011.

29 Prokopenko, M. G., Hirst, M., DeBrabandere, L., Lawrence, D., Berelson, W. M., Granger, J.,
30 Chang, B., Dawson, S. C., Crane III, E., Chong, L., Thamdrup, B., Townsend-Small, A., and
31 Sigman, D. M.: Nitrogen losses in anoxic marine sediments driven by Thioploca-anammox
32 bacteria consortia, *Nature*, 500, 194-198, doi:10.1038/nature12365, 2013.

33 Rabalais, N. N.: Nitrogen in Aquatic Environments, *Ambio*, 31, 102-112, 2002.

34 Rao, A. M., and Charette, M. A.: Benthic nitrogen fixation in a eutrophic estuary affected by
35 groundwater discharge *Journal of Coastal Research*, 28, 477-485, 2012.

36 Ren, H., Sigman, D. M., Thunell, R. C., and Prokopenko, M. G.: Nitrogen isotopic composition
37 of planktonic foraminifera from the modern ocean and recent sediments, *Limnology and*
38 *Oceanography*, 57, 1011-1024, 2012.

39 Risgaard-Petersen, N.: Coupled nitrification-denitrification in autotrophic and
40 heterotrophic estuarine sediments: On the influence of benthic microalgae, *Limnology and*
41 *Oceanography*, 48, 93-105, 2003.

42 Røy, H., Kallmeyer, J., Adhikari, R. R., Pockalny, R., Jorgensen, B. B., and D'Hondt, S.: Aerobic
43 microbial respiration in 86-million-year-old deep-sea red clay, *Science*, 336, 922-925,
44 doi:10.1126/science.12119424, 2012.

1 Rutgers van der Loeff, M., Meadows, P., and Allen, J.: Oxygen in porewaters of deep-sea
2 sediments [and Discussion], *Philosophical Transactions of the Royal Society B*, 331, 69-84,
3 1990.

4 Rysgaard, S., Risgaard-Petersen, N., Nielsen, L. P., and Revsbech, N. P.: Nitrification and
5 Denitrification in Lake and Estuarine Sediments Measured by the ^{15}N Dilution Technique
6 and Isotope Pairing, *Applied and Environmental Microbiology*, 59, 2093-2098, 1993.

7 Sachs, O., Sauter, E., Schlüter, M., Rutgers van der Loeff, M. M., Jerosch, K., and Holby, O.:
8 Benthic organic carbon flux and oxygen penetration reflect different plankton provinces in
9 the Southern Ocean Deep Sea Research Part I: *Oceanographic Research Papers*, 56, 1319-
10 1335, 2009.

11 Seeberg-Elverfeldt, J., Schlüter, M., Feseker, T., and Kölling, M.: Rhizon sampling of
12 porewaters near the sediment-water interface of aquatic systems, *Limnology and*
13 *Oceanography: Methods*, 3, 361-371, 2005.

14 Seitzinger, S. P., Nixon, S. W., and Pilson, M. E. Q.: Denitrification and nitrous oxide
15 production in a coastal marine ecosystem, *Limnology and Oceanography*, 29, 73-83, 1984.

16 Shearer, G. B., Schneider, J. D., and Kohl, D. H.: Separating the efflux and influx components
17 of net nitrate uptake by *Synechococcus* R2 under steady-state conditions, *Journal of*
18 *General Microbiology*, 137, 1179-1184, 1991.

19 Sigman, D. M., Casciotti, K. L., Andreani, M., Barford, C., Galanter, M., and Böhlke, J. K.: A
20 Bacterial Method for the Nitrogen Isotopic Analysis of Nitrate in Seawater and Freshwater,
21 *Analytical Chemistry*, 73, 4145-4153, 2001.

22 Sigman, D. M., Granger, J., DiFiore, P. J., Lehmann, M. F., Ho, R., Cane, G., and van Geen, A.:
23 Coupled nitrogen and oxygen isotope measurements of nitrate along the eastern North
24 Pacific margin, *Global Biogeochemical Cycles*, 19, GB4022, doi:10.1029/2005GB002458,
25 2005.

26 Sigman, D. M., DiFiore, P. J., Hain, M., Deutsch, C., Wang, Y., Karl, D. M., Knapp, A. N.,
27 Lehmann, M. F., and Pantoja, S.: The dual isotopes of deep nitrate as a constraint on the
28 cycle and budget of oceanic fixed nitrogen, *Deep Sea Research I*, 56, 1419-1439,
29 doi:10.1016/j.dsr.2009.04.007, 2009.

30 Usui, T., Koike, I., and Ogura, N.: N_2O Production, Nitrification and Denitrification in an
31 Estuarine Sediment, *Estuarine and Coastal Shelf Science*, 52, 769-781, 2001.

32 Wada, E., Kadonaga, T., and Matsuo, S.: ^{15}N abundance in nitrogen of naturally occurring
33 substances and global assessment of denitrification from isotopic viewpoint, *Geochemical*
34 *Journal*, 9, 139-148, 1975.

35 Wankel, S. D., Kendall, C., Pennington, J. T., Chavez, F. P., and Paytan, A.: Nitrification in the
36 euphotic zone as evidenced by nitrate dual isotopic composition: Observations from
37 Monterey Bay, California, *Global Biogeochemical Cycles*, 21, GB2009, Artn Gb2009Doi
38 10.1029/2006gb002723, 2007.

39 Wankel, S. D., Kendall, C., and Paytan, A.: Using nitrate dual isotopic composition ($\delta^{15}\text{N}$ and
40 $\delta^{18}\text{O}$) as a tool for exploring sources and cycling of nitrate in an estuarine system: Elkhorn
41 Slough, California, *Journal of Geophysical Research*, 114, G01011,
42 doi:10.1029/2008JG000729, 2009

43 Wankel, S. D., Mosier, A. C., Hansel, C. M., Paytan, A., and Francis, C. A.: Spatial variability in
44 nitrification rates and ammonium oxidizing microbial communities in the agriculturally
45 impacted Elkhorn Slough estuary, California, *Applied and Environmental Microbiology*, 77,
46 269-280, 2011.

- 1 Wenk, C. B., Zopfi, J., Brees, J., Veronesi, M., Niemann, H., and Lehmann, M. F.: Community N
2 and O isotope fractionation by sulfide-dependent denitrification and anammox in a
3 stratified lacustrine water column, *Geochimica et Cosmochimica Acta*, 125, 551-563,
4 doi:10.1016/j.gca.2013.10.034, 2014.
- 5 Zhang, X., Sigman, D. M., Morel, F. M. M., and Kraepiel, A. M. L.: Nitrogen isotope
6 fractionation by alternative nitrogenases and past ocean anoxia, *Proceedings of the*
7 *National Academy of Sciences of the United States of America*, 111, 4782-4787, 2014.
- 8 Zhao, R. and Jørgensen, S.L.: Microbial nitrogen cycling in oligotrophic sediments from the
9 Mid Atlantic Ridge, *ISME Journal*, in review.
- 10 Ziebis, W., McManus, J., Ferdeman, T., Schmidt-Schierhorn, F., Bach, W., Muratli, J., Edwards,
11 K. J., and Villinger, H.: Interstitial fluid chemistry of sediments underlying the North Atlantic
12 Gyre and the influence of subsurface fluid flow, *Earth and Planetary Science Letters*, 323-
13 324, 79-91, 2012.
- 14 Zumft, W. G.: Cell biology and molecular basis of denitrification, *Microbiology and*
15 *Molecular Biology Reviews*, 61, 533-616, 1997.
- 16

Figure 1

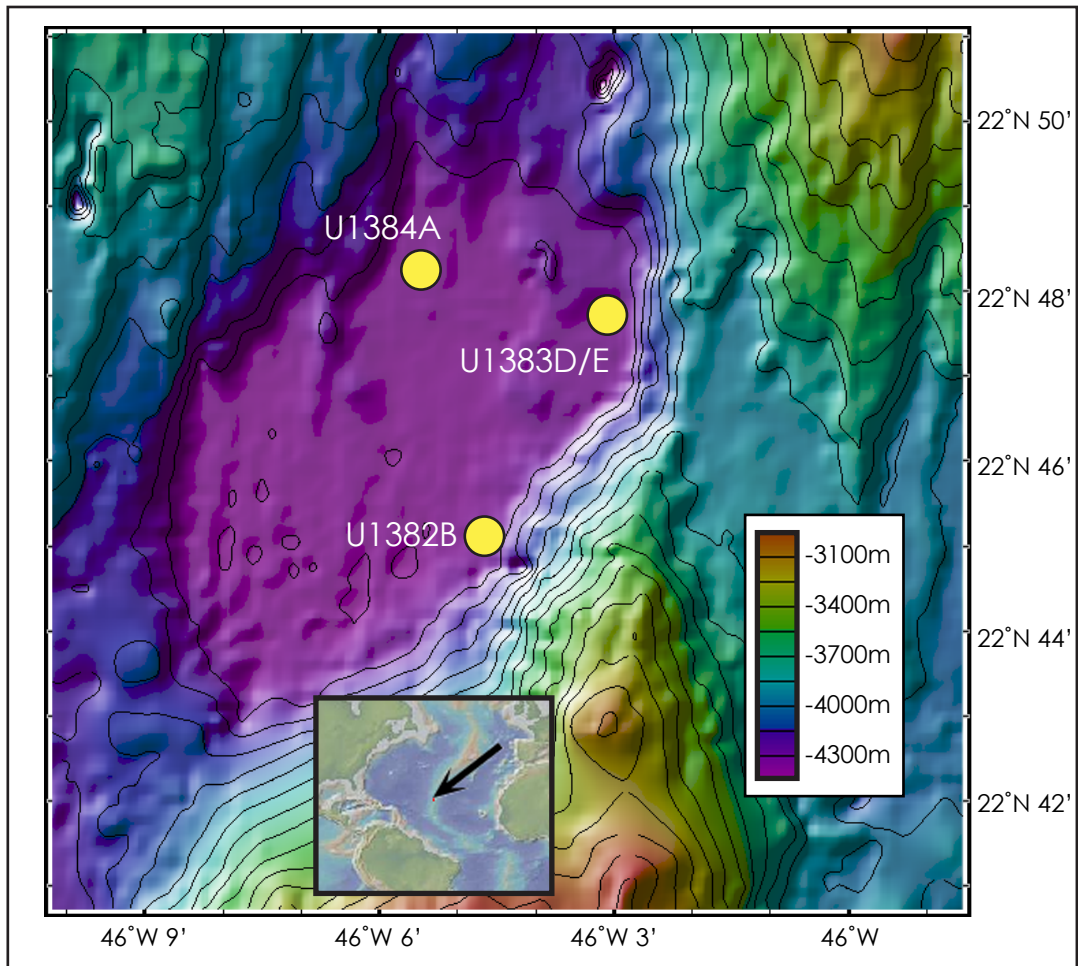


Figure 2

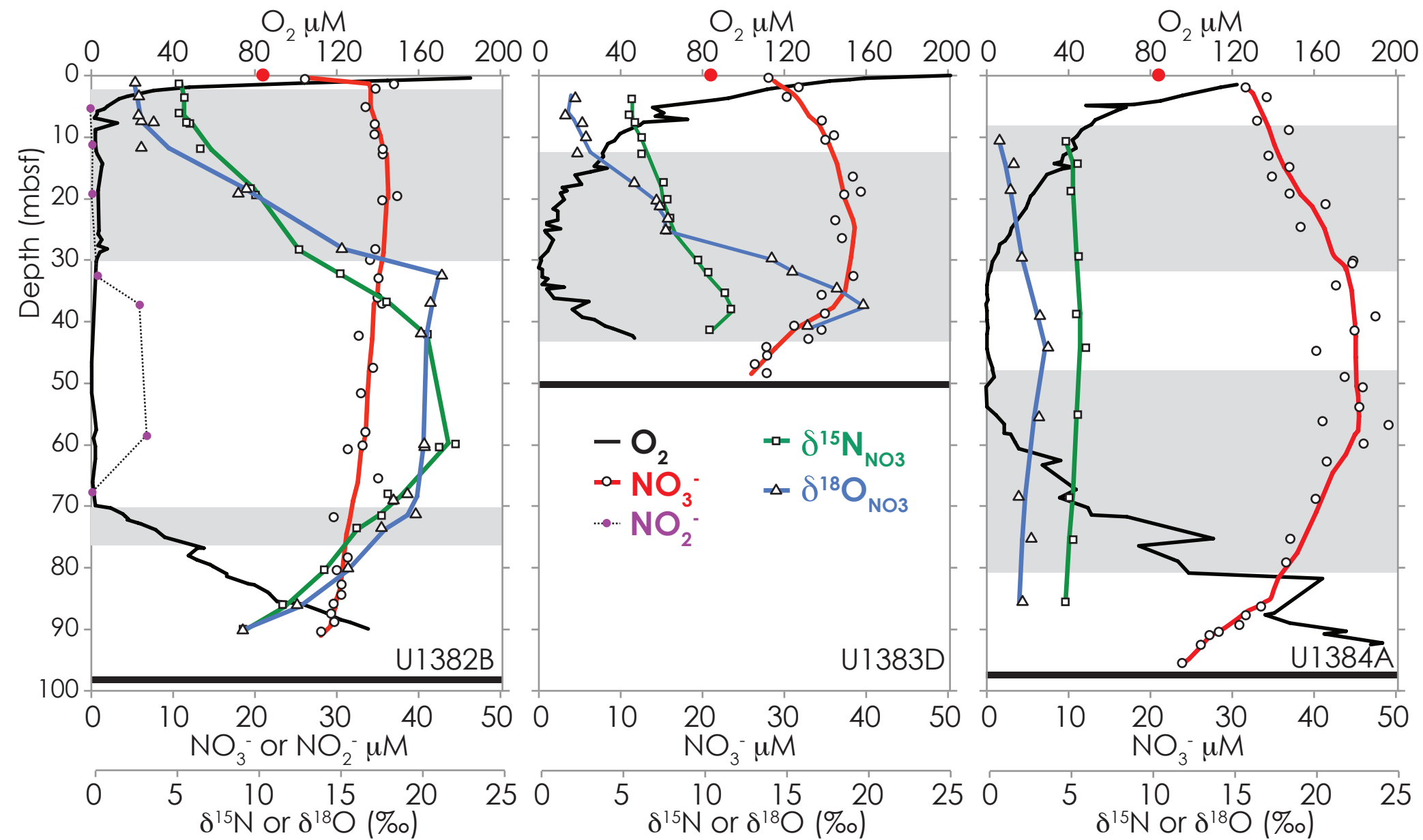


Figure 3

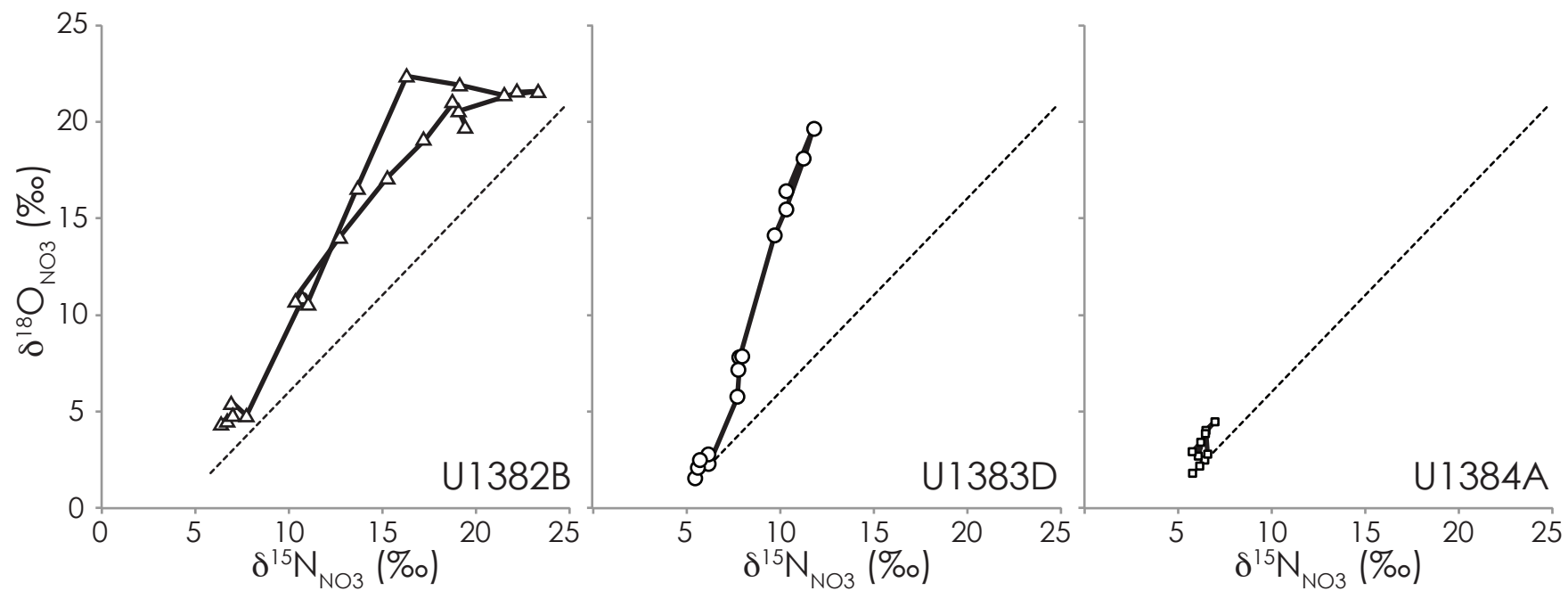


Figure 4

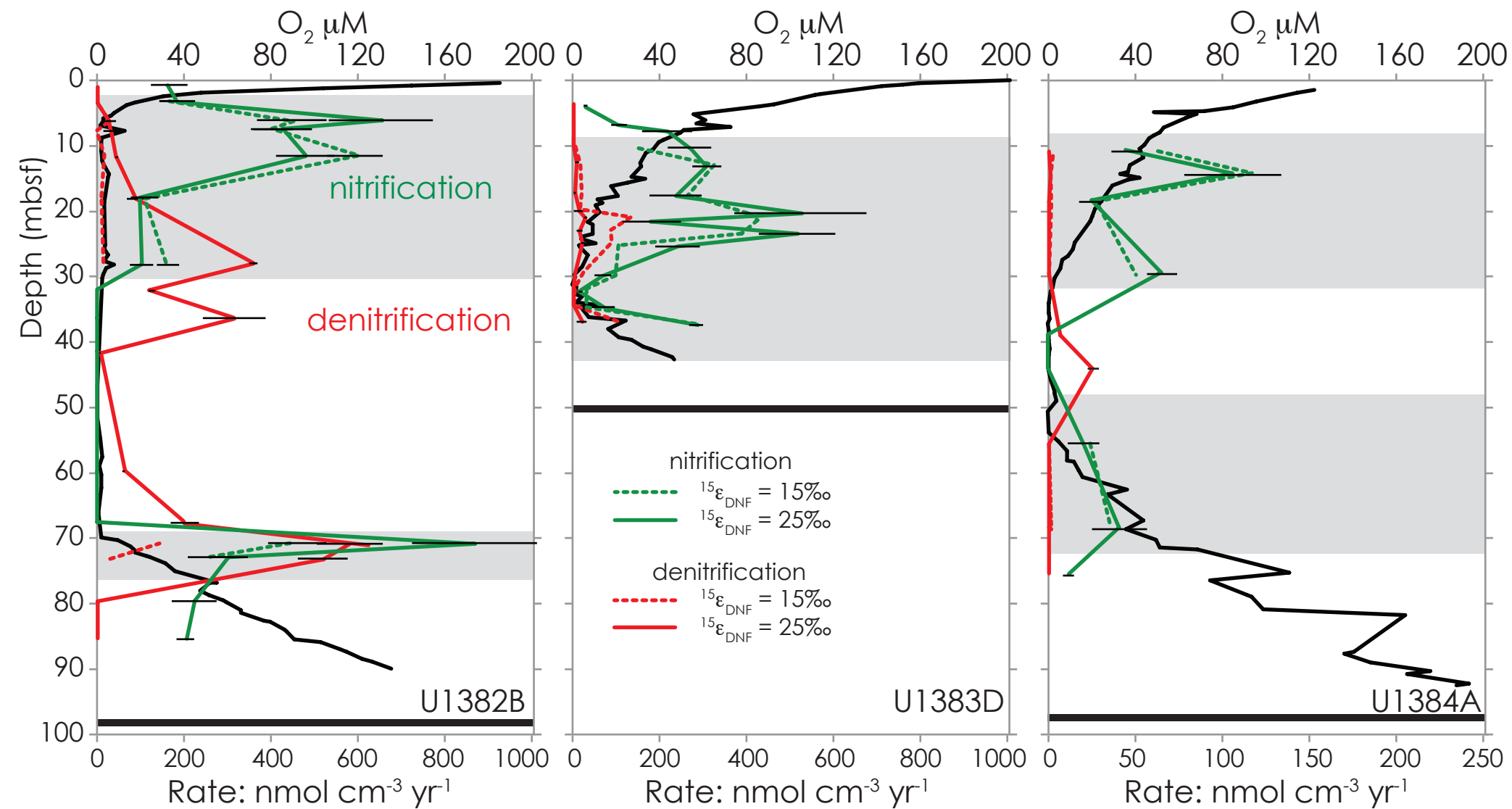


Figure 5

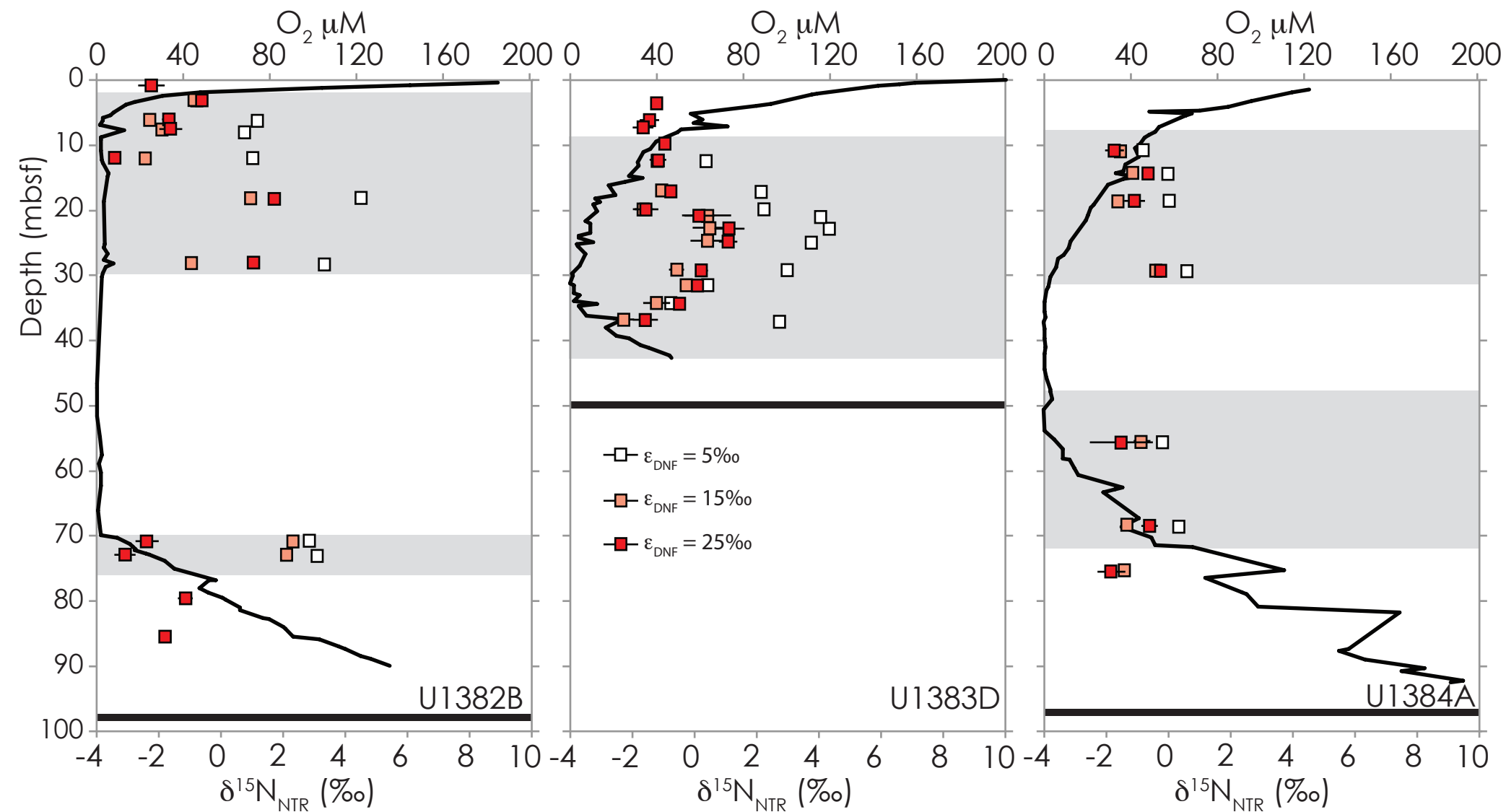


Figure 6

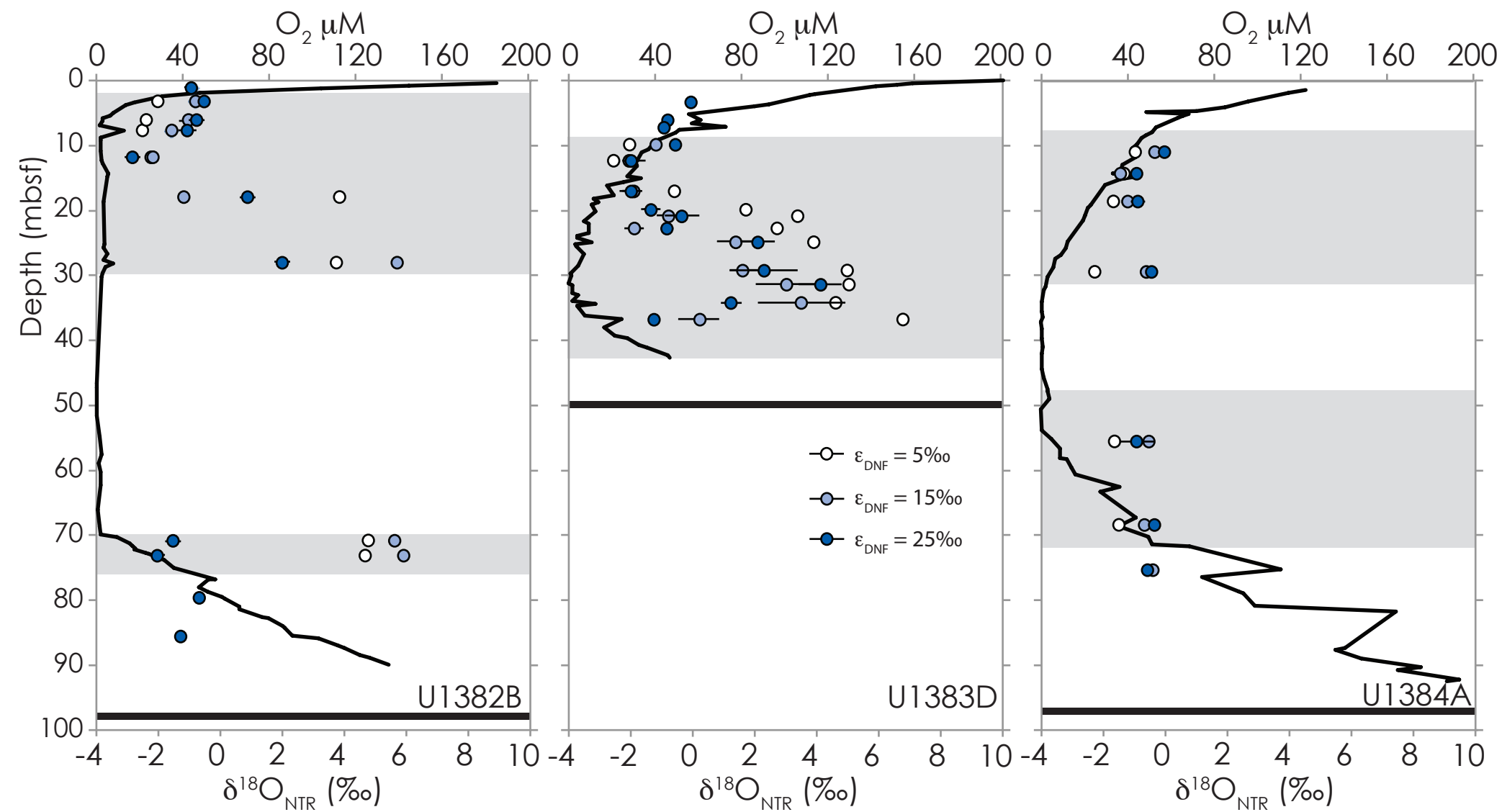


Table 2. Denitrification isotope effects $^{15}\epsilon_{\text{DNF}}$ and $^{18}\epsilon:^{15}\epsilon_{\text{DNF}}$ estimated from anoxic porewaters at North Pond

Denitrification Parameters

Core ID	Depth mbsf	$^{15}\epsilon_{\text{DNF}}$			$^{18}\epsilon:^{15}\epsilon_{\text{DNF}}$		
U1382B	32.1	21.0	±	0.3	0.99	±	0.02
U1382B	36.3	21.9	±	0.4	0.95	±	0.02
U1382B	41.6	20.7	±	0.1	0.84	±	0.01
U1382B	59.8	18.8	±	0.3	1.07	±	0.02
U1382B	67.7	17.4	±	0.4	1.11	±	0.02
U1384A	38.8	*	±	*	*	±	*
U1384A	44.1	8.1	±	0.2	1.08	±	0.04

*changes in $\delta^{15}\text{N}$ and $\delta^{18}\text{O}$ were too small over this interval for resolving a reliable estimate of $^{15}\epsilon$ or $^{18}\epsilon:^{15}\epsilon$